18. *Electromagnetic Induction within the Earth and Its Relation to the Electrical State of the Earth's Interior. Part I* (2)*

By Tsuneji RIKITAKE,

Earthquake Research Institute.

(Read Mar. 18, Apr. 16 and Sept. 16, 1947.—Received Sept. 18, 1947.)

CHAPTER VI. ELECTROMAGNETIC INDUCTION BY MAGNETIC VARIATION CONNECTED WITH SOLAR ERUPTION.

1. Radio fade-outs and magnetic variations connected with solar chromospheric eruptions.

On the basis of many data collected in the years 1935 and 1936, Dellinger[52] showed that sudden fade-outs of radio signals reflected from the ionosphere (the so-called Dellinger-effect) used to be accompanied by magnetic effects of special character. Meanwhile, according to solar observations, it was reported that many bright chromospheric eruptions were accompanied by the fade-outs reported by Dellinger. It is very likely, that, at the time of solar eruption, H-alpha light sent from the sun causes remarkable changes in the ionization of the ionosphere, especially in or just below the E-layer, and consequently the absorption of electric waves and variation in the earth's magnetic field both take place.

Although it is beyond the scope of this paper to discuss the general aspects of solar eruption and its allied phenomena, a brief description of the magnetic effect will be given here.

The magnetic effects connected with solar eruptions are of different type from the other magnetic disturbances such as bay-type disturbance, pulsation and sudden commencement of magnetic storm. According to magnetographic records accumulated up to this time, the disturbance begins suddenly reaching its maximum within several or scores of *minutes* and then decreases gradually.

---

*) Being continued from p. 98 of the Bulletin Vol. 28 parts 1-2 (1950).

52) J. H. DELLINGER, *Terr. Mag.* 42 (1937), 49.

Its maximum magnitude usually amounts to scores of *gammas*. It seldom lasts over one *hour*. Changes in vertical intensity are generally small compared with that of the horizontal components.

As to the distribution of the disturbing forces, examination of the records from many observatories shows that nothing takes place at observatories situated in the dark hemisphere while magnetic effects at observatories situated in the sun-lit hemisphere are considerable. According to Fleming[53] and McNish[54), 55] who investigated the atmospheric current-systems by which the magnetic effect may be caused, it was established that the direction of this change roughly agreed with those of the diurnal variation expected at that time and the magnitude was roughly proportional to the magnitude of the diurnal variation departure. McNish showed clearly this character in several figures concluding that the magnetic effect accompanying the solar eruption is an augumentation of S_q. It is reasonable, when we bear the "dynamo"-theory of S_q in mind, that the increase in the electric conductivity of the ionosphere due to the abnormal ionization caused by the solar eruption permits an increase in the electric current-intensity then flowing.

Although the mechanism of occurrence of the magnetic effects accompanying the solar eruption was investigated rather lately, the existence of such magnetic variations was already known at the early period of this century. Birkeland[39] showed a kind of magnetic disturbance called "Cyclo-median storm." The magnetograms from many observatories showed clearly the same character as mentioned above. In spite of the fact that the relations to the solar phenomena and the fade-out were unknown at that time, we may presume that Birkeland's "Cyclo-median storm" was a magnetic effect associated with the solar eruption.

2. The analysis of the magnetic variation accompanied by solar eruption.

Since the disturbing forces of the magnetic variation caused by a solar eruption are not measurable in the dark hemisphere, while they increase towards the sub-solar point in the other hemisphere, it is obvious that a large number of spherical harmonics is needed to make an approximation of the field with a spherical harmonic expansion. In that case, accordingly, we must have more complete data from well-distributed observatories to make a spherical harmonic analysis than in the case of S_q in which we could express the field fairly well with only a few harmonic functions.

53) J. A. FLEMING, *Terr. Mag.* 41 (1936), 404.
54) A. G. MCNISH, *Terr. Mag.* 42 (1937), 109.
55) A. G. MCNISH, *Nature* 139 (1937), 244.

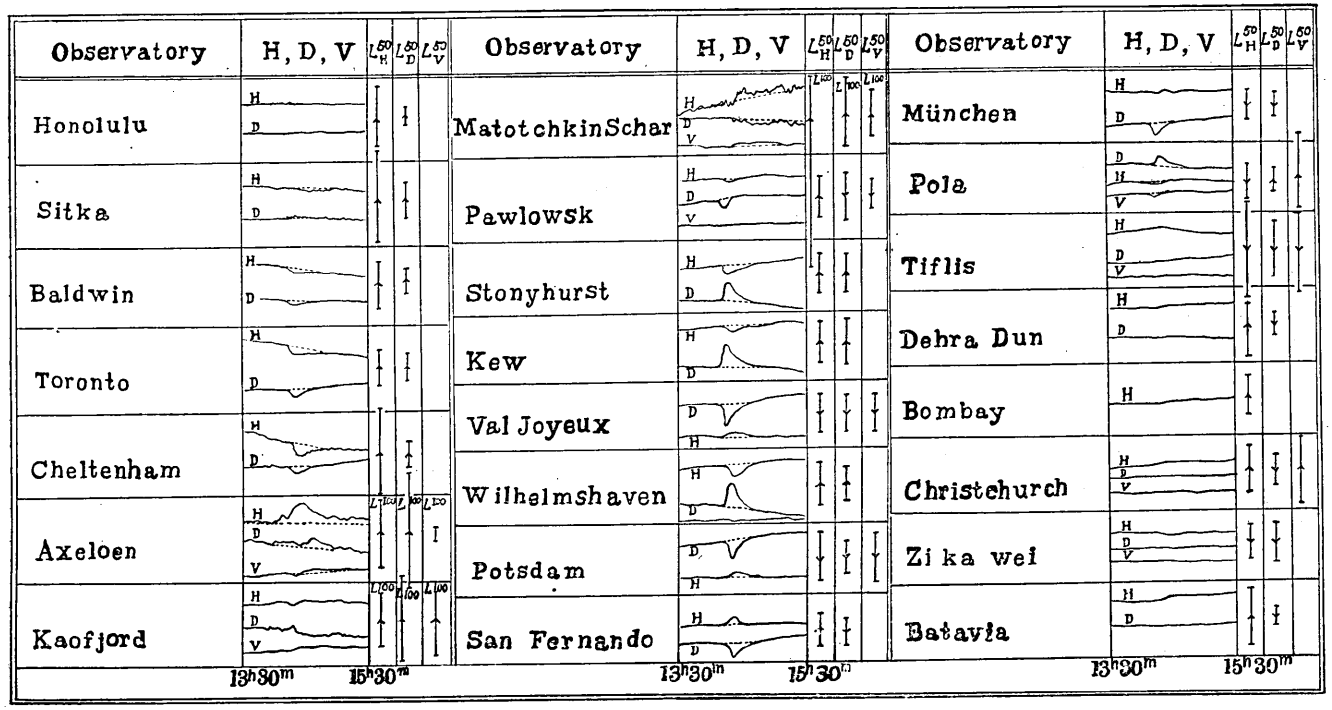

Fig. 25. The disturbance of Oct. 6, 1932. The scale value is given graphically by lines placed at the end of each curve. At the head of the column are the signs L_h^n, L_d^n and L_v^n, which indicate the length of a deflection in **H**, **D** and **V** respectively, corresponding to direction of increasing horizontal intensity, increasing westerly declination, and increasing vertical intensity. (After Birkeland)

Unfortunately, however, the writer could not get sufficient data for that purpose. So far the writer could get, only Birkeland's[39] data for the magnetic variation of Oct. 6, 1902 were utilizable including magnetograms from 23 observatories. But, on account of lack of observatories in the oceans, as in other cases of the magnetic variation caused by solar eruption, it seems almost impossible to make a spherical harmonic analysis having many higher harmonics. For this reason, we shall treat the problem as one observed on a plane surface in European Region in which we have comparatively many stations.

Table XIX.

The perturbing forces on the 6th October, 1902. (After K. Birkeland)

G.M.T.	Baldwin		Cheltenham		Toronto		Axeloren		
	Ph	*Pd*	*Ph*	*Pd*	*Ph*	*Pd*	*Ph*	*Pd*	*Pv*
h m									
14 15	−1.6 γ	E 3.9 γ	0	W 0.6 γ	−2.2 γ	E 0.6 γ	+ 8.1 γ	W 0.3 γ	+ 2.4 γ
18.8	−3.5	10.2	− 6.0 γ	E 6.5	−6.4	12.3	+16.5	E 0.6	+19.7
22.5	−4.4	8.7	−11.1	12.7	−7.1	14.4	+22.5	2.0	+17.2
26.3	−3.4	6.5	− 9.7	8.6	−2.6	8.5	+24.5	0.1	0
30	−2.0	5.0	− 7.5	5.6	−4.7	4.8	+23.5	W 1.1	−14.8
33.8	−1.1	3.0	− 5.9	5.2	−3.2	2.6	+16.4	4.6	−19.7
37.5	−0.6	2.5	− 4.1	2.4	−1.9	1.7	+11.2	6.4	−14.8
41.3	−0.1	1.3	− 2.7	0.8	−0.7	0	+ 7.1	4.9	−12.3
45	0	0.4	− 1.3	0.2	0	0	+ 4.5	2.6	− 9.8

Table XIX (continued)

G.M.T.	Kaafjord			Pawlowsk			Stonyhurst		Wilhelmshaven		
	Ph	*Pd*	*Pv*	*Ph*	*Pd*	*Pv*	*Ph*	*Pd*	*Ph*	*Pd*	*Pv*
h m											
14 15	−2.9 γ	W 3.3 γ	0	−0.5 γ	W 5.5 γ		−5.6 γ	W 9.4 γ	0	W 1.9 γ	0
18.8	−3.1	5.5	+1.1 γ	−5.5	5.5	A slight	−13.0	23.5	−6.2 γ	31.3	0
22.5	−1.9	0.5	+5.0	−5.0	2.8	pertur-	−11.8	17.2	−13.1	28.3	−3.0 γ
26.3	+0.7	E 1.4	+7.2	−2.0	0.9	bation;	− 9.8	11.8	−12.7	16.6	−5.5
30	+1.0	2.2	+6.2	−1.0	0.5	*Pv* max	− 8.2	7.8	− 8.2	9.6	−4.0
33.8	+1.2	3.0	+6.2	−1.0	0	= +3.7γ	− 6.7	4.7	− 5.2	4.9	0
37.5	+1.0	2.8	+6.2	−0.5	0	at about	− 5.4	2.7	− 2.9	2.2	0
41.3	+0.2	2.7	+5.5	0	0	14*h* 24*m*	− 4.5	1.5	− 1.1	0.4	0
45	0	1.5	+1.0	0	0		− 3.9	0.8	− 0.6	0	0

Table XIX (continued)

G. M. T.	Kew		Potsdam			Val Joyeux		
	Ph	*Pd*	*Ph*	*Pd*	*Pv*	*Ph*	*Pd*	*Pv*
h *m*								
14 15	0	W16.1 γ	−0.6 γ	W10.4 γ	−0.6 γ	−2.1 γ	W 8.2 γ	
18.8	−4.4 γ	24.3	−4.4	25.5	0	−3.2	16.2	Perhaps
22.5	−7.1	17.3	−5.8	16.2	+0.6	−3.5	14.4	a slight
26.3	−7.5	11.4	−5.1	9.6	+0.6	−3.5	7.9	neg.
30	−6.2	8.2	−3.6	4.9	0	−3.3	5.3	deflection.
33.8	−4.8	5.4	−2.3	2.6	0	−3.1	3.4	The curve
37.5	−4.4	3.8	−1.7	1.0	0	−2.5	2.1	somewhat
41.3	−4.1	2.8	−1.1	0	0	−2.3	1.4	indistinct.
45	−3.5	2.1	−0.7	0	0	−1.8	0.8	

Table XIX (continued)

G. M. T.	Münich		Pola			San Fernando	
	Ph	*Pd*	*Ph*	*Pd*	*Pv*	*Ph*	*Pd*
h *m*							
14 15	+2.0 γ	W15.0 γ	+0.4 γ	0		0	0
18.8	+2.5	30.0	+1.8	W13.1 γ		+10.4 γ	W 27.2 γ
22.5	0 (*)	19.5	+3.9	22.7	From 14 *h* 16 *m* to	+10.3	25.9
26.3	0 (*)	11.3	+3.0	15.1	14 *h* 28 *m* a slight	+ 4.5	14.9
30	+11.0 (*)	7.5	+0.4	9.3	perturbation in V.	+ 1.2	9.9
33.8	+3.0 (*)	3.8	+0.2	5.2	At 14 *h* 20 *m*	+ 0.5	6.2
37.5	0	2.2	0	2.6	*Pv* max. = −2.1.	0	3.2
41.3	0	0	0	1.0		0	1.5
45	0	0	0	0		0	0.7

(*) The curious form of the H-curve is due to a certain work going on in the Observatory at the time. The corresponding values of *Ph* are therefore rather uncertain.

The copies of the magnetographic records collected by Birkeland are reproduced in Fig. 25. The deviations from the normal curves which are shown in the figure with broken lines were also obtained by Birkeland at several times during the course of the variation as tabulated in Table XIX. The horizontal disturbing forces at 14 *h* 22.5 *m* GMT (nearly the time of maximum variation) in European Region are shown in Fig. 26 while the magnitudes in vertical intensity were reported from only five observatories, Kaafjord, Pawlowsk, Wilhelmshaven, Potsdam and Pola as shown in Fig. 28.

Taking into account the similarity of the field-distribution to that of S_q, we may draw equal variation line of X and Z as illustrated in Figs. 27 and 28.

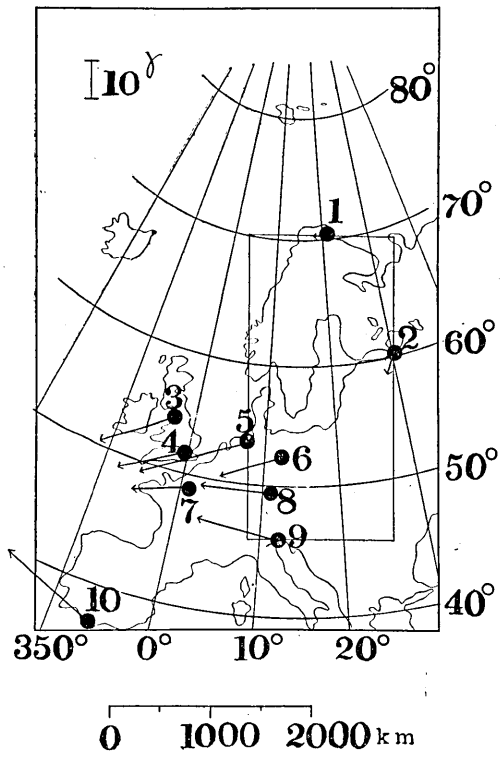

Fig. 26. The horizontal disturbing forces at 14 h 22.5 m.
1. Kaafjord. 2. Pawlowsk. 3. Stonyhurst. 4. Kew. 5. Wilhelmshaven. 6. Potsdam. 7. Val-Joyeux. 8. Münich. 9. Pola. 10 San Fernand.

In order to include five stations from which variation in the vertical intensity was reported, we shall study the rectangular area, as also shown in Fig. 26, with sides approximately 3000×1500 km. Owing to the shortage, however, of available data we shall merely estimate the first harmonic by means of Fourier analysis or practically least squares.

The magnetic potential of the variation is generally expressed as follows;

$$W=\sum_m \sum_n (c_{mn}e^{-kz}+i_{mn}e^{kz}) \begin{matrix}\cos\\ \sin\end{matrix} mx \begin{matrix}\cos\\ \sin\end{matrix} ny\,, \quad \text{.....(2.1)}$$

where

$$k^2=m^2+n^2\,. \quad \text{.....(2.2)}$$

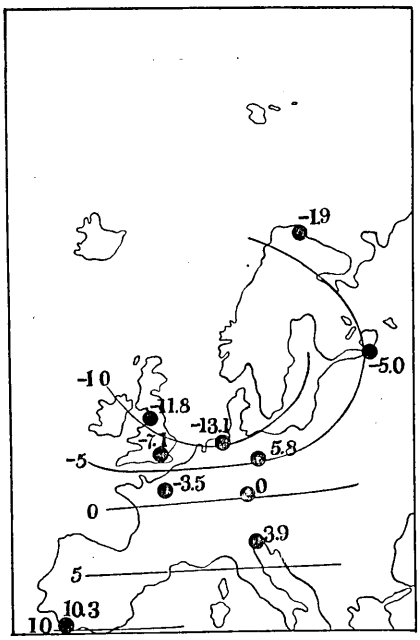

Fig. 27. Equal variation line for the north component at 14 *h* 22.5 *m*. (Unit: γ)

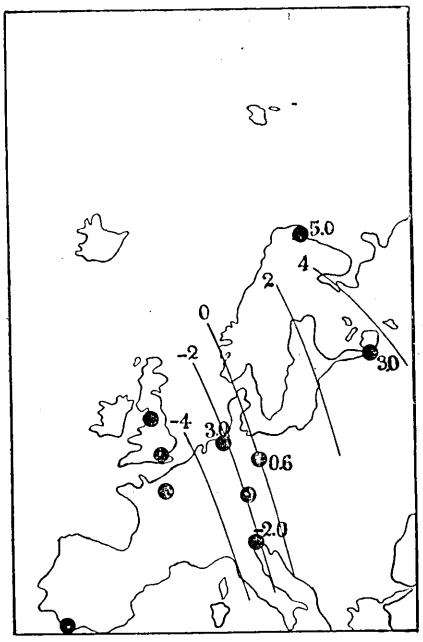

Fig. 28. Equal variation line for the vertical component at 14 *h* 22.5 *m*. (Unit: γ)

If we take x, y and z to the directions north-, east- and downwards, the terms involving negative indices of exponential correspond to the potential originating above the earth and positive indices to that within the earth. In that case, the components of the magnetic field are given by

$$\left.\begin{aligned} X &= -\sum_m \sum_n (e_{mn}e^{-kz} + i_{mn}e^{kz}) \frac{\partial V_{mn}}{\partial x}, \\ Y &= -\sum_m \sum_n (e_{mn}e^{-kz} + i_{mn}e^{kz}) \frac{\partial V_{mn}}{\partial y}, \\ Z &= -\sum_m \sum_n k\,(-e_{mn}e^{-kz} + i_{mn}e^{kz})\, V_{mn}, \end{aligned}\right\} \quad \text{.....(2.3)}$$

writing V_{mn} in place of the harmonic functions in (2.1). Then we get on the earth's surface

$$\left.\begin{aligned} X &= -\sum_m \sum_n (e_{mn} + i_{mn}) \frac{\partial V_{mn}}{\partial x}, \\ Y &= -\sum_m \sum_n (e_{mn} + i_{mn}) \frac{\partial V_{mn}}{\partial y}, \\ Z &= -\sum_m \sum_n k\,(-e_{mn} + i_{mn})\, V_{mn}, \end{aligned}\right\} \quad \text{.....(2.4)}$$

by putting $z=0$.

On the other hand, we get from the analysis of the observed data

$$\left.\begin{aligned} X&=-\sum_m\sum_n a_{mn}\frac{\partial V_{mn}}{\partial x},\\ Y&=-\sum_m\sum_n b_{mn}\frac{\partial V_{mn}}{\partial y},\\ Z&=-\sum_m\sum_n c_{mn}V_{mn}. \end{aligned}\right\} \quad \cdots\cdots(2.5)$$

Hence, equating the corresponding coefficients in the series of X and Z in (2.4) and (2.5), we have

$$e_{mn}+i_{mn}=a_{mn},$$
$$k(-e_{mn}+i_{mn})=c_{mn}.$$

Solving this we get

$$\left.\begin{aligned} e_{mn}&=\frac{a_{mn}-c_{mn}/k}{2},\\ i_{mn}&=\frac{a_{mn}+c_{mn}/k}{2}. \end{aligned}\right\} \quad \cdots\cdots(2.6)$$

Thus we can separate the coefficients of the magnetic potential into the external and internal parts. The same determination can also be done combining Y and Z.

In the case of the magnetic variation concerned here, the coefficients of $\frac{L}{\pi}\sin\frac{\pi}{L}x$ in Y and $\frac{L}{\pi}\cos\frac{\pi}{L}x$ in Z are determined at nine times during the course of the variation. L denotes the length of the sides parallel to x axis. Applying, then, the above mentioned theory, the coefficients of the magnetic potential are obtained as shown in Table XX and Fig. 29. As

Table XX. The coef. of the magnetic potential.

Coef. \ Time	14*h*15*m*	18·8 *m*	22·5 *m*	26·3 *m*	30 *m*	33·8 *m*	37·5 *m*	41·3 *m*	45 *m*
$-e$	−0·4γ	3·2	6·6	6·5	4·3	2·7	2·5	1·3	0·4
$-i$	−0·5	2·1	2·8	2·0	0·3	0·1	−0·2	−0·8	0·0

pointed out by Birkeland himself, since the variation at Kaafjord seemed to be affected by local irregularities during later periods in which $\triangle Z$ at Kaafjord amounted to several *gammas* while $\triangle Z$ was not measurable at other stations, the determined coefficients after 14 *h* 30 *m* seem to be less reliable.

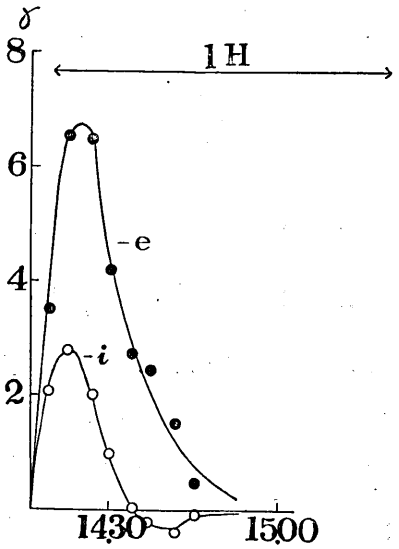

Fig. 29. The coefficients of the magnetic potential.

3. Theory of plane-earth induction and its relation to the electrical state of the earth's interior.

We shall discuss the electromagnetic induction within the plane-earth as shown in Fig. 30 where the superficial layer with thickness D is non-conducting while the deeper region has specific conductivity σ.

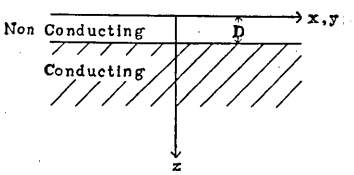

Fig. 30.

In the non-conducting region, the magnetic potential exists as is given by (2.1) having the components of the magnetic field expressed by (2.3). Meanwhile, we have vector potential $\vec{A}$ in the conducting region which satisfies in quasi-stationary state

$$\nabla^2\vec{A}=4\pi\sigma\frac{\partial\vec{A}}{\partial t}, \qquad \text{.....(3.1)}$$

provided $\mu=1$. Putting p in place of $\partial/\partial t$, (3.1) becomes in operational form

$$(\nabla^2-\kappa^2)\vec{A}=0, \qquad \kappa^2=4\pi\sigma p \text{ .....(3.2), (3.3)}$$

The solution of (3.2) which is sufficient for the present problem is given by

$$\vec{A}=C_{mn}e^{-\sqrt{k^2+\kappa^2}\,z}\,[\vec{r}\,\mathrm{grad}\,V_{mn}], \qquad \text{.....(3.4)}$$

where C_{mn} denotes a function of p. The terms involving positive indices of expotential must not be taken into account because they become infinite at $z \to \infty$.

Then with the aid of the relation $\vec{B}=\text{rot}\,\vec{A}$, we get the components of the magnetic field as follows;

$$\left.\begin{aligned} X &= -C_{mn}\sqrt{k^2+\kappa^2}\, e^{-\sqrt{k^2+\kappa^2}\, z}\frac{\partial V_{mn}}{\partial x}, \\ Y &= -C_{mn}\sqrt{k^2+\kappa^2}\, e^{-\sqrt{k^2+\kappa^2}\, z}\frac{\partial V_{mn}}{\partial y}, \\ Z &= C_{mn}k^2 e^{-\sqrt{k^2+\kappa^2}\, z} V_{mn}. \end{aligned}\right\} \quad \text{.....(3.5)}$$

In order to satisfy the boundary conditions at $z=D$ where the continuity in the magnetic field must be held, we get from (2.3) and (3.5)

$$\left.\begin{aligned} e\, e^{-kD}+i\, e^{kD} &= C\sqrt{k^2+\kappa^2}\, e^{-\sqrt{k^2+\kappa^2}\, D}, \\ e\, e^{-kD}-i\, e^{kD} &= Cke^{-\sqrt{k^2+\kappa^2}\, D}. \end{aligned}\right\} \quad \text{.....(3.6)}$$

abbreviating suffices m and n. Solving (3.6) we have

$$i(t)=I(p)\, e(t), \qquad I(p)=e^{-2kD}\frac{\sqrt{k^2+\kappa^2}-k}{\sqrt{k^2+\kappa^2}+k} \quad \text{.....(3.7)}$$

by which we can estimate the change in the induced field when the inducing field is given.

As shown by Price[7] and already used in the previous chapter, we have

$$\begin{aligned} i(t) &= \frac{d}{dt}\int_0^t e(t-u)\, h(u)\, du \\ &= e(t)\, h(0)+\int_0^t e(t-u)\, h'(u)\, du \quad \text{.....(3.8)} \end{aligned}$$

where $h(t)$ corresponds to $i(t)$ when $e(t)=0$ $(t<0)$ and $=1$ $(t>0)$. $h(u)$, then, is given by the contour integration

$$h(u)=\frac{1}{2\pi i}\int_L e^{tu} I(p)\frac{dp}{p} \quad \text{.....(3.9)}$$

where L is Bromwich's path of integration having all sigularities in its left-hand-side on the complex plane.

At present, there is only one branch-point at $-\frac{k^2}{4\pi\sigma}$, real and negative. Then, the integration along L is equivalent to that as is shown in Fig. 31 in

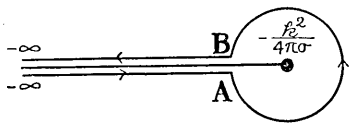

Fig. 31.

which a cut is made in the Riemann surface with straight line from $-\frac{k^2}{4\pi\sigma}$ to $-\infty$. With this convention the integrand is one-valued and analytic. Hence the integrals along $(-\infty)A$ and $B(-\infty)$ become respectively

$$\int_{(-\infty)A} = e^{-2kD}\int_{\infty}^{\frac{k^2}{4\pi\sigma}} e^{-qu}\frac{\sqrt{k^2-4\pi\sigma q}+k}{\sqrt{k^2-4\pi\sigma q}-k}\frac{dq}{q},$$

$$\int_{B(-\infty)} = e^{-2kD}\int_{\frac{k^2}{4\pi\sigma}}^{\infty} e^{-qu}\frac{\sqrt{k^2-4\pi\sigma q}-k}{\sqrt{k^2-4\pi\sigma q}+k}\frac{dq}{q},$$

and consequently

$$\int_{(-\infty)A} + \int_{B(-\infty)} = \frac{k}{\pi\sigma}e^{-2kD}\int_{\frac{k^2}{4\pi\sigma}}^{\infty}\frac{\sqrt{k^2-4\pi\sigma q}}{q^2}e^{-qu}\,dq.$$

Writing then β^2 in place of $q-\frac{k^2}{4\pi\sigma}$, we get

$$\int_{(-\infty)A} + \int_{B(-\infty)} = i8a\,e^{-2kD-\frac{k^2}{4\pi\sigma}u}\int_0^{\infty} e^{-u\beta^2}\frac{\beta^2 d\beta}{(\beta^2+\frac{k^2}{4\pi\sigma})^2}\cdot\left(a^2=\frac{k^2}{4\pi\sigma}\right)$$

Meanwhile, the integral round the small circle AB vanishes when the radius of the circle reaches zero. Thus we get

$$h(u)=\frac{4a}{\pi}e^{-2kD-\frac{k^2}{4\pi\sigma}u}\int_0^{\infty} e^{-u\beta^2}\frac{\beta^2 d\beta}{(\beta^2-\frac{k^2}{4\pi\sigma})^2}\cdot \quad \text{.....(3.10)}$$

By this expression, we can calculate $h(u)$ at any value of u with the aid of numerical integration.

On the other hand, however, we have more convenient expression for small value of u. Expanding $I(p)$ in a series of descending power of p, we obtain

$$I(p)=e^{-2kD}\left(1-2\sqrt{\frac{k^2}{4\pi\sigma}}\,p^{-\frac{1}{2}}-2\frac{k^2}{4\pi\sigma}p^{-1}\cdots\cdots\right) \quad \text{.....(3.11)}$$

whence

$$h(u)=e^{-2kD}\left(1-\frac{2k}{\pi\sqrt{\sigma}}\sqrt{u}-\frac{k^2}{\pi\sigma}u\cdots\cdots\right) \quad \text{.....(3.12)}$$

for small value of u.

For instance, $h(u)$ is obtained in four case, $D=200\,km$ $\sigma=5\times10^{-12}emu$, $D=200\,km$ $\sigma=10^{-13}emu$, $D=400\,km$ $\sigma=5\times10^{-12}emu$ and $D=400\,km$ $\sigma=10^{-13}emu$ as shown in Fig. 32.

$i(t)$, then may be obtained by integrating numerically (3.8). But, to a fair degree of approximation, $h'(u)$ is regarded as a constant for the small value of u when the process of calculation becomes easier. $i(t)$ which corresponds to $e(t)$ given by Table XX are calculated in the four cases mentioned above being shown in Fig. 33 together with the values obtained from the analysis. As easily seen in the figure, the cases in which D is assumed to be 200 *km* give larger values in the maximum amplitude than the values obtained from the observation while the cases in which D is assumed to be 400 *km* give roughly suitable values in their maximum magnitudes, decaying, however, more rapidly in the case $\sigma=10^{-13}$ *emu* and more slowly in the case $\sigma=5\times10^{-12}$ *emu*. Then we may approximately consider that D amounts to about 400 *km* and σ amounts to the order of 10^{-12}*emu* to make the results of theory agree with those of the analysis.

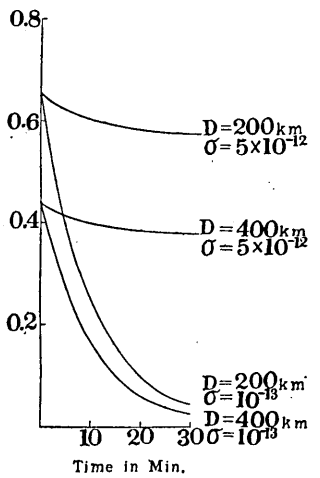

Fig. 32. $h(t)$ for various cases.

It is very interesting that the study of the magnetic variation which accompanies solar eruption shows us nearly the same electrical structure in the earth's interior which was already obtained in the cases of S_q, S_D, D_{st} and bay-type disturbance.

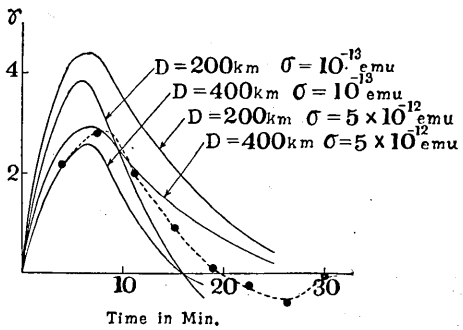

Fig. 33. The induced field expected from theory in various cases and the result from analysis (broken line).

Although in the present study the conductivity in the conducting region seems rather low, when compared with that obtained in the case of S_q, discussions about such detail will prove fruitless because we have only one example in this chapter and consequently can say nothing about the accuracy of the determination of the coefficients. Hence the present study merely shows that there are no serious objections to the electrical state of the earth's interior which was previously studied, leaving for the future more accurate research on the induction by the magnetic variation connected with solar eruption.

4. The distribution of the induced currents.

As the relation between the current-density $\vec{c}$ and the vector potential $\vec{A}$ is given by

$$\vec{c} = -\sigma \frac{\partial \vec{A}}{\partial t}, \quad \cdots\cdots(4.1)$$

substituting (3.4) in (4.1), we have in operational form

$$\vec{c} = -\sigma p C(p)\, e^{-\sqrt{k^2+\kappa^2}z}\, e(t)\, [\vec{r}\,\mathrm{grad} V_{mn}], \quad \cdots\cdots(4.2)$$

where $C(p)$ is given by the solution of the simultaneous equations (3.6) as

$$C(p) = \frac{2e^{-(k-\sqrt{k^2+\kappa^2})D}}{k+1/\sqrt{k^2+\kappa^2}} \quad \cdots\cdots(4.3)$$

Taking into consideration, then, that $e(t)$ in Fig. 31 is expressible, to a fair degree of approximation, by

$$e(t) = Ate^{-\omega t}\,(t>0), \qquad =0\,(t<0)$$

preferring suitable values for A and ω ($A=-5{\cdot}1\times10^{-2}\gamma$, $\omega=2{\cdot}8\times10^{-3}\,sec^{-1}$). The operational form of $e(t)$ is given by

$$e(t) = \frac{Ap}{(p+\omega)^2} H(t), \quad \cdots\cdots(4.4)$$

where $H(t)$ denotes Heaviside's unit function.

Hence the coefficient of $[\vec{r}\,\mathrm{grad}\, V_{mn}]$ in (4.2) can be written as follows;

$$c(t) = -2A\sigma e^{-kD} \frac{e^{-\sqrt{k^2+\kappa^2}(z-D)}}{k+1/\sqrt{k^2+\kappa^2}} \frac{p^2}{(p+\omega)^2} H(t) \quad \cdots\cdots(4.5)$$

The solution of the operational equation (4.5), as often studied in the previous chapters, is given by a contour integral of the type

$$c(t) = -\frac{A\sigma e^{-kD}}{\pi i}\int_L \frac{e^{-\sqrt{k^2+\kappa^2}(z-D)}}{k+1/\sqrt{k^2+\kappa^2}} \frac{p}{(p+\omega)^2} e^{pt}\, dp, \quad \cdots\cdots(4.6)$$

where L is Bromwich's path of integration having all singularities on its left-hand-side. Then, taking into consideration the fact that we have a branch-point at $-\frac{k^2}{4\pi\sigma}$ and a double pole at $-\omega$, both real and negative ($\omega > \frac{k^2}{4\pi\sigma}$ in this case), the integration along L becomes equivalent with that along a contour, as shown in Fig. 34, where, making a cut with a straight line connecting $-\infty$ to the branch-point, the integrand is one-valued and analytic.

For the sake of brevity, however, we shall neglect to describe in detail the process of integration. Taking into consideration that $\int_{CD}$ vanishes when the radius attains to zero while $\int_{AB}+\int_{EF}$ does not, we get

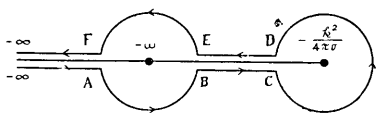

Fig. 34.

$$c(t)=-A\sigma e^{-kD}\left[\left\{\frac{d}{dp}\frac{e^{pt-\sqrt{k^2+4\pi\sigma p}\,(z-D)}}{k+\sqrt{k^2+4\pi\sigma p}}\right\}_{p=-\omega}\right.$$

$$\left.-\frac{e^{-\frac{k^2t}{4\pi\sigma}}}{\pi^2\sigma}\int_0^\infty \frac{k\sin\sqrt{4\pi\sigma}(z-D)\beta+\sqrt{4\pi\sigma}\beta\cos\sqrt{4\pi\sigma}(z-D)\beta}{\left(\beta^2+\frac{k^2}{4\pi\sigma}-\omega\right)^2}e^{-t\beta^2}\beta d\beta\right]$$

.....(4.7)

A more convenient expression for small value of t is also obtained in a similar way with (4.12) and (4.13), Chapter V. As to large value of p we get from (4.5)

$$c(t)\simeq -A\sqrt{\frac{\sigma}{\pi}}\,e^{-kD}(1/\sqrt{p}\,)\,e^{-(z-D)\sqrt{4\pi\sigma p}}\,H(t)\,.\,.\,.\,.\,.\,.\,.\,.(4.8)$$

Solving (4.8), we have

$$c(t)\simeq -2\sigma Ae^{-kD}\left\{\frac{1}{\pi}\sqrt{\frac{t}{\sigma}}\,e^{-\frac{\pi\sigma(z-D)^2}{t}}-(z-D)\left(1-\mathrm{erf.}\,(z-D)\sqrt{\frac{\pi\sigma}{t}}\right)\right\}$$[56]

.....(4.9)

Taking, then, $\sigma=10^{-12}emu$, $t=360\,sec$, $D=400\,km$ and $k=\frac{\pi}{L}=1.05\times10^{-8}\,cm^{-1}$, the change in the current-density with depth is calculated as shown in Fig. 35 on an arbitrary scale. As seen in the figure the decay of the induced currents is so rapid that they become practically zero at the depth of 100 km beneath the surface of the core.

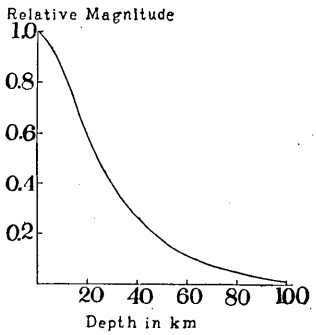

Fig. 35. The distribution of the induced currents in the earth.

At the depth of z, consider, a current-sheet of infinitesimal thickness. The intensity of its own magnetic field just outside its surface is determined solely by the value and distribution of current-density $\vec{c}$ in the sheet. The magnetic field at any depth z_0 varies as $e^{-k(z-z_0)}$. Hence at the earth's surface the magnetic field

56) See footnote (18), Chapter V.

due to the current-sheet is proportional to $|\overrightarrow{c}|e^{-kz}$. Thus we calculate the contribution of the currents of various depth to the magnetic field at the earth's surface, being expressed by almost the same curve with the current-distribution shown in Fig. 35 because the range of the depth in which the currents are flowing is comparatively small compared with its depth measured from the earth's surface.

In short, we may say that the determined conductivity corresponds to that just below the surface of the uniform core.

CHAPTER VII ELECTROMAGNETIC INDUCTION BY SUDDEN COMMENCEMENT OF MAGNETIC STORM.

1. The world-wide distribution of sudden commencements.

It is well known that magnetic storms often begin abruptly with an increase in horizontal intensity. In almost all cases, sudden changes stop within several minutes. Thus, it is of interest to study electromagnetic induction by such rapid variation in order to make clear the electrical state of the earth's interior in conjunction with slower variations already studied in the preceding chapters.

According to the investigations[57], [58], [59], [60], [61], [62], [63], [64], up to this time, sudden commencement occurs almost simultaneously all over the earth with an increase in horizontal intensity, while the changes in vertical intensity and declination depend on circumstances. On the basis of data collected by Bauer[58], as reproduced in Tables XXI, XXII and XXIII, some characters of this sudden commencement will be subsequently examined.

In the first place, we find as a whole that the order of magnitudes of increases in horizontal intensity or ΔH is roughly maintained throughout all storms, that is to say, the increases in horizontal intensity at some stations where the increases are larger or smaller than at other stations in case of storm seem

57) L. A BAUER, *Terr. Mag.* 16 (1911), 85 and 163.
58) L. A. BAUER, *Terr. Mag.* 15 (1910), 9 and 219.
59) L. A. BAUER, and W. J. PETERS, *Terr. Mag.* 30 (1925), 45.
60) L. RODÉS, *Terr. Mag.* 27 (1922) 161.
61) G. ANGENHEISTER, *Nachrichten Ges. Wiss. Göttingen, Math.-Phys. Klasse*, 4 (1913) 565.
62) R. L. FARIS, *Terr. Mag.* 15 (1910) 93, 213 and 16 (1911), 109.
63) A. TANAKADATE, *Assemblée de Lisbonne* (1933), *Int. Geod. Geophys. Union, Associaiton Magn. Electr. Terr.* p. 149.
64) W. ELLIS, *Proc. Roy. Soc. London* 102 (1892) 191.

Table XXI ΔH in γ (After L. A. Bauer)

Observatory	Geomagn. Latitude	Geomagn. Longitude	No. 1	No. 2	No. 3	No. 4	No. 5	No. 6	No. 7	No. 8	No. 9	No. 10	No. 11	No. 12	No. 13	No. 14	No. 15
Sitka	60·0	275·4	−12·9	12·9	27·3	23·0	19·1	16·5	—	47·2	29·3	105·5	37·2	—	113·0	10·9	64·2
Stonyhurst	57·0	82·5	57	25	40	59	30	25	—	45	—	150	10	78	85	−17	—
Copenhagen	55·7	98·6	—	—	—	—	45	—	—	—	6	136	−25	62	—	17	—
Greenwich	54·2	83·8	65	24	45	63	35	6	—	41	11	130	6	79	37	22	—
Kew	54·0	83·3	57	22	35	42	41	10	53	38	8	112	7	75	72	20	−420
Falmouth	54·0	77·9	50	19	34	55	20	10	34	37	6	100	6	60	65	19	—
Uccle	52·7	87·8	40	18	36	32	34	8	48	32	−6	110	−8	49	57	15	−354
Potsdam	52·5	97·1	−6	4	61	50	40	5	61	32	5	147	−14	64	55	12	21
Cheltenham	50·1	350·5	−23·5	8·7	10·0	23·2	18·0	17·7	−23·7	49·6	23·7	15·5	25·2	74·2	97·5	3·9	—
Baldwin	48·9	328·5	36·9	6·3	50·1	18·0	15·8	25·9	15·8	47·2	26·0	6·8	31·1	41·0	97·8	9·1	−150
Ekaterinburg	48	40	40	19	45	32	9	10	58	10	—	—	−6	35	15	5	17
München	48	93	39	14	43	22	26	13	31	30	5	90	4	47	51	9	−261
Pola	45·1	94·4	32·5	15·0	45·0	20·0	35·0	17·5	40·7	30·5	—	101·8	5·1	45·8	61·0	15·3	−262·1
Porto Rico	29·6	3·9	22·1	3·1	17·2	7·0	7·1	13·8	12·0	13·9	4·9	16·5	13·5	26·1	72·0	2·1	114
Helwan	27·2	106·4	—	—	—	—	25	25	35	29	19	115	26	45	72	26	86
Honolulu	21·1	266·5	19·4	8·6	42·3	18·5	18·4	14·1	15·1	18·6	19·0	21·7	22·0	30·2	55·0	2·5	95
Zi-ka-wei	19·9	189·5	24	12	63	34	34	20	—	19	22	93	16	34	68	21	143
Bombay	9·5	143·6	26	7	65	19	29	22	32	15	20	119	18	23	67	22	101
Samoa	−16·0	260·2	19·2	6·0	32·4	19·2	—	14·9	13·4	18·8	15·1	23·0	19·6	25·3	—	—	—
Batavia	−18·0	175·6	35	9	13	48	37	25	37	22	25	53	21	36	—	25	—
Pilar	−20·2	4·6	—	—	66	38	25	24	−28	8	16	50	22	57	35	25	54
Mauritius	−26·6	122·4	22	7	49	9	17	17	11	18	14	16	60	8	23	42	47

Table XXII ΔZ in γ (After L. A. Bauer)

Observatory	No. 1	No. 2	No. 3	No. 4	No. 5	No. 6	No. 7	No. 8	No. 9	No. 10	No. 11	No. 12	No. 13	No. 14	No. 15
Sitka	6·2	−0·6	8·7	0	7·9	4·7	—	5·1	3·7	20·3	3·8	—	34·5	3·0	—
Stonyhurst	—	—	—	—	—	—	—	—	—	—	—	—	—	—	—
Copenhagen	—	—	—	—	10	—	—	—	—	31	−7	14	—	—	—
Greenwich	9	0	0	17	0	4	9	4	−4	17	−4	13	9	4	—
Kew	10	5	—	10	0	6	20	6	0	0	0	0	10	0	—
Falmouth	8	0	4	8	2	1	18	5	−2	14	−2	6	4	2	—
Uccle	—	—	—	15	—	—	—	—	—	11	—	12	18	12	—
Potsdam	2	−1	−7	−2	−5	−5	−5	−5	−1	−27	−2	−7	−7	−3	−27
Cheltenham	−2·5	−1·6	2·9	−4·5	−4·8	1·9	−5·4	−1·6	1·2	6·0	0·9	−4·3	−5·5	0	−14·7
Baldwin	−3·4	−2·0	−3·0	3·0	−2·0	0	−11·2	7·6	−1·0	10·6	—	−5·0	−2·4	−1·2	−39
Ekaterinburg	2	5	−3	1	3	0	0	1	—	—	−3	−3	1	1	−9
München	—	—	—	—	—	—	—	—	—	—	—	—	—	—	—
Pola	—	—	—	9·6	—	9·6	—	−4·4	—	4·4	−24·0	9·6	−19·2	—	−16·9
Porto Rico	—	−2·5	15·4	−16·3	7·1	6·1	11·0	7·1	6·2	5·7	14·7	—	28·0	4·2	56·3
Helwan	—	—	—	—	−9	−12	−12	−12	−9	−39	−12	—	−24	−9	—
Honolu'u	3·7	4·4	4·2	5·1	8·4	4·8	8·4	5·3	6·2	11·2	6·4	13·4	16·9	—	6·5
Zi-ka-wei	−2	−1	—	−10	—	−3	—	—	—	—	−3	−6	−7	−2	−26
Bombay	−4	0	−12	−1	−5	−4	−6	−2	−3	−14	−2	−3	−15	−2	−20
Samoa	—	—	—	—	4·5	4·7	—	—	2·9	5·8	3·0	4·0	—	—	—
Batavia	3	2	—	—	—	—	5	—	—	0	−7	2	—	3	36
Pilar	—	—	−2·8	−9·7	−1·0	−1·0	1·0	0·3	0·8	−1·9	−0·7	0·8	1·3	0·6	4·0
Mauritius	−9	−1	−13	−3	—	—	—	−2	−14	—	−6	−7	—	—	−50

Table XXIII Δt in *min.* (After L. A. Bauer)

Observatory	No. 1	No. 2	No. 3	No. 4	No. 5	No. 6	No. 7	No. 8	No. 9	No. 10	No. 11	No. 12	No. 13	No. 14	No. 15
Sitka	2·0	1·2	1·2	0·8	1·5	3·0	—	3·6	3·6	—	3·3	—	—	—	—
Stonyhurst	1·5	4	0·5	1	1	2	—	4	—	—	2	2	6	—	—
Copenhagen	—	—	—	—	—	—	—	—	—	—	—	—	—	—	—
Greenwich	—	7	4	—	—	—	—	—	—	—	—	—	5	—	—
Kew	2	7	4	2	4	1	12	5	1	—	1	1	5	—	—
Falmouth	2	10	3	1	1	1	3	3·5	0·5	—	—	4	6	—	—
Uccle	3	5·4	3·1	1·2	5·4	5·0	—	4·6	3·1	—	1·0	1·9	7·7	—	—
Potsdam	0·8	1·5	4·5	3·0	1·2	0·6	4·5	3·6	0·8	—	1·5	1·5	6·0	—	—
Cheltenham	0·5	1·5	0·6	0·8	0·8	2·4	0·8	3·7	3·6	—	2·4	3·0	9·0	—	—
Baldwin	3·0	1·2	1·8	0·8	1·0	3·6	0·6	4·5	3·9	—	3·6	4·5	6·0	—	—
Ekaterinburg	2·5	2·7	3·8	1·2	0·8	0·8	1·6	0·7	—	—	0·0	0·4	0·8	—	—
München	3·0	9·0	7·5	2·0	1·3	7·0	4·5	5·5	3·0	—	0·1	2·8	7·0	—	—
Pola	1·5	6·0	4·0	3·0	4·5	8·0	12·0	3·0	—	—	1·0	0·5	8·0	—	—
Porto Rico	0·9	2·1	1·5	0·8	0·9	4·5	1·5	2·4	3·6	—	4·5	1·8	9·9	—	—
Helwan	—	—	—	—	2	2	5	3	2	—	8	2	6	—	—
Honolulu	4·5	3·0	2·0	1·8	1·8	3·0	2·1	4·5	2·2	—	5·1	0·6	9·6	—	—
Zi-ka-wei	5	3	10	2	7	5	—	5	2	—	2	1	13	—	—
Bombay	4·0	2·5	9·2	1·8	6·3	6·8	3·8	4·0	3·5	—	6·3	1·5	10·7	—	—
Samoa	7	5	2	1	—	4	1	3	3	—	6	1	—	—	—
Batavia	3·9	2·4	3·0	4·0	4·0	4·0	3·6	4·2	3·6	—	2·4	3·0	—	—	—
Pilar	—	—	1·6	1·2	4·0	6·8	4·8	2·0	6·5	—	5·2	2·0	6·0	—	—
Mauritius	1	6	3	2	8	6	9	8	4	—	2	1	8	—	—

to be always larger or smaller at any time than those of the respective stations. For instance, taking the increase of No. 4 as abscissa and those of Nos. 2 and 13 as ordinate, we find that the relations mentioned above hold good in the main as shown respectively in Figs. 36 and 37.

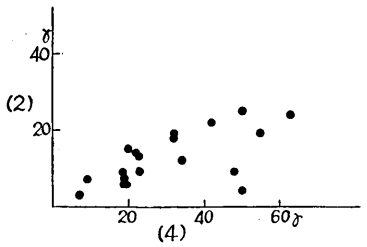

Fig. 36. Abscissa: ΔH for No. 4.
Ordinate: ΔH for No. 2.

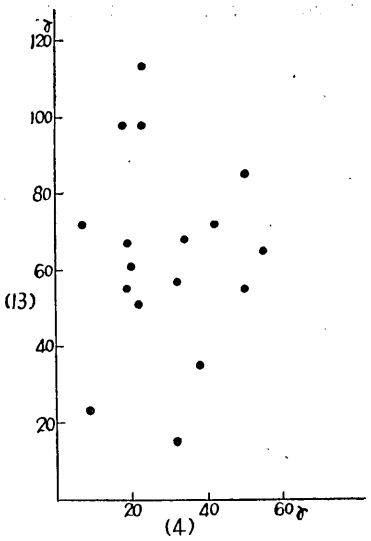

Fig. 37. Abscissa: ΔH for No. 4.
Ordinate: ΔH for No. 13.

In the second place, similar tendency is found in the changes in vertical intensity or ΔZ as shown in Figs. 38 and 39.

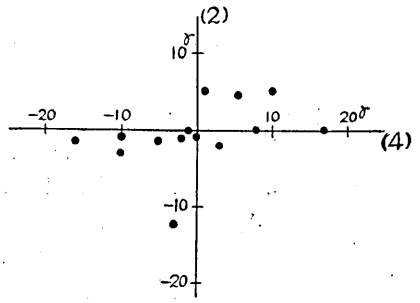

Fig. 38. Abscissa: ΔZ for No. 4.
Ordinate: ΔZ for No. 2.

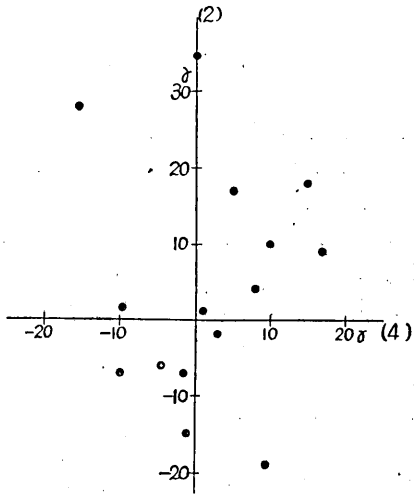

Fig. 39. Abscissa: ΔZ for No. 4.
Ordinate: ΔZ for No. 13.

In the third place, the duration-time of sudden commencements or Δt measured from the beginning to the first turning point is rather long in some storms in all the stations while in other storm it is comparatively short. Such relations, for instance, are shown in Figs. 40 and 41 in which Δt's of No. 2 and No. 13 are plotted against that of No. 4 with respect to each observatory.

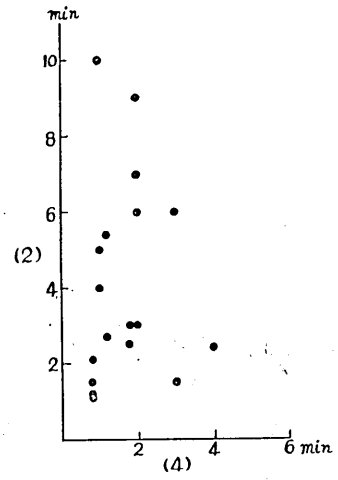

Fig. 40. Abscissa: Δt for No. 4.
Ordinate: Δt for No. 2.

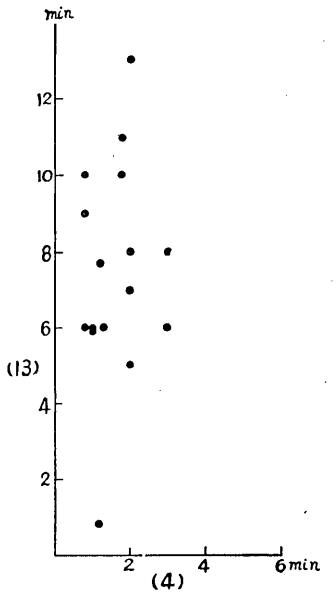

Fig. 41. Abscissa: Δt for No. 4.
Ordinate: Δt for No. 13.

Though the points in these figures seem comparatively scattered, the above-mentioned relations seem to hold roughly.

In order to avoid irregularities, we shall discuss about the averaged character. Mean values of ΔH and ΔZ are given in Table XXIV while that of Δt amounts to about 3 *minutes*. The storms No. 10, No. 11, No. 14 and No. 15 are excluded from the average because the determination of these quantities seems rather ambiguous in these four cases. The distribution of the mean values of ΔH and ΔZ referred to the geomagnetic latitude are illustrated in Fig. 42. Although data in southern hemisphere are scarce, it seems that ΔH becomes large near the auroral zones and the geomagnetic equator, while ΔZ, though not so clearly, changes its sign at the geomagnetic equator. As fully studied in the investigation on the main phase of magnetic storm, these characters suggest that the sudden commencement is caused by the effect

Table XXIV. Mean value of ΔH and ΔZ.

Observatory	ΔH (γ)	ΔZ (γ)
Sitka	39	7
Stonyhurst	46	—
Copenhagen	38	6
Greenwich	37	5
Kew	38	6
Falmouth	33	4
Uccle	28	—
Potsdam	30	−4
Cheltenham	25	−2
Baldwin	34	−2
Ekaterinburg	24	1
München	27	—
Pola	32	−6
Porto Rico	18	7
Honolulu	23	7
Zi-ka-wei	31	−5
Bombay	29	−5
Samoa	18	4
Batavia	28	1
Pilar	26	−1
Mauritius	21	7

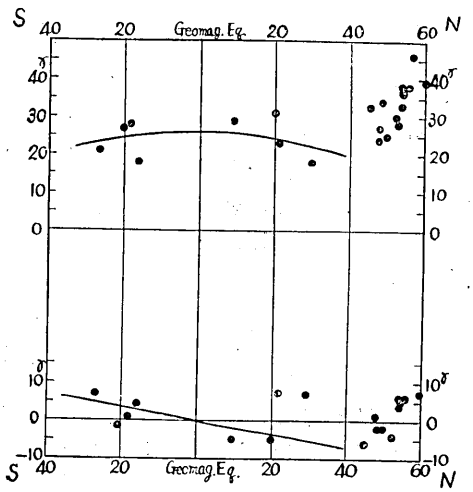

Fig. 42. The distribution of mean values of ΔH (upper) and ΔZ (lower) referred to geomagnetic coordinate. The curves show the first harmonic components in the low and middle latitude.

equivalent to the electric current concentrating above the auroral zones and the equator.

2. The analysis of sudden commencements.

As shown in Fig. 42, the greatest part of the magnetic potential of the variation can be expressed with the term including $P_1(\cos\theta)$, where θ denotes geomagnetic colatitude, the high latitudes being excluded. Limitting our discussions to the low and middle latitudes, we shall estimate the coefficients of the components of the magnetic field as follows. Taking into consideration the fact that the changes in declination are usually small, we may approximately regard ΔH as the changes in geomagnetic north component ΔX. Using the data from observatories distributed between 30°N and 30°S except Honolulu and Porto Rico[65], the coefficients of $\sin\theta$ and $\cos\theta$ respectively in ΔX and ΔZ are obtained by means of least squares in every storm being shown in Table XXV.

Table XXV Coefficients in γ.

Coef. \ Storm	No. 1	No. 2	No. 3	No. 4	No. 5	No. 6	No. 7	No. 8	No. 9	No. 11	No. 12	No. 13
$-\Delta H$	26	8·2	47	26	26	21	25	19	19	26	34	61
$-\Delta Z$	6·1	3·2	25	15	11	10	8·7	3·2	4·5	9·5	11	17

In that case, the magnetic potential of the variation can be expressed by

$$R\left(e\frac{r}{R}+i\frac{R^2}{r^2}\right)P_1(\cos\theta),$$

where R denotes the radius of the earth. e and i denote respectively the coefficients originating above and within the earth. Then the magnetic field at the surface are given by

$$\left.\begin{aligned}\Delta X&=-(e+i)\sin\theta,\\ \Delta Z&=(e-2i)\cos\theta.\end{aligned}\right\} \quad \text{.....(2.1)}$$

Thus combining ΔX and ΔZ which are given in Table XXV, e and i are obtained from (2.1) as tabulated in Table XXVI together with the ratio e/i.

65) The changes at both observatories are remarkably different from the general tendency, especially in vertical intensity. According to the writer's opinion, this may be due to the influence of the sea as will be studied later.

Table XXVI Coef. of the external and internal parts in γ.

Storm	No. 1	No. 2	No. 3	No. 4	No. 5	No. 6	No. 7	No. 8	No. 9	No. 11	No. 12	No. 13
$-e$	19	6·5	40	22	21	17	20	14	14	21	26	46
$-i$	6·7	1·7	7·3	3·7	5·0	3·7	5·3	5·3	4·7	5·3	7·7	15
e/i	2·8	3·8	5·5	5·9	4·2	4·6	3·8	2·6	3·0	4·0	3·4	3·1

Thus the most probable value of e/i becomes 3.9 ± 0.2. It is to be noted that e/i is considerably large when compared with that of any other variation studied before.

3. The relation to the electrical state of the earth's interior.

According to the theories of electromagnetic induction within a uniformly conducting sphere, the coefficient of the n-th order harmonics of the magnetic potential i_n originating within that sphere, as already studied in the previous chapters, is given by the operational equation of the type

$$i_n = I(p)\, e_n(t), \quad \text{.....(3.1)}$$

where e_n denotes the corresponding coefficient of the inducing field originating out of the sphere.

$I(p)$ was already obtained in (3.3), Chapter V, being given as

$$I(p) = \frac{q^3}{2}\left\{1 - \frac{F_1(\sqrt{4\pi\sigma p}qa)}{F_0(\sqrt{4\pi\sigma p}qa)}\right\} \quad \text{.....(3.2)}$$

in the case $n=1$ where a and q denote respectively the radius of the sphere on whose surface the magnetic field is observed and the ratio of the radius of the conducting sphere to that of the former. F_0 and F_1 were already known[66].

The mode of the change in the external part differs from each other in every storm concerned. However, the gradient of change is steeper at the beginning, decreasing gradually with the lapse of time. For the sake of mathematical convenience, we assume that $e(t)$ goes on as

$$\left.\begin{aligned} e(t) &= A(1-e^{-\alpha t}) \quad (t>0), \\ &= 0 \qquad\qquad (t<0). \end{aligned}\right\} \quad \text{.....(3.3)}$$

66) See the footnote on p. 95.

Preferring a suitable value to α, the course of assumed $e(t)$ is shown in Fig. 43. Writing (3.3) in operational form, we get

$$e(t)=\frac{A\alpha}{p+\alpha}H(t) \quad \cdots\cdots(3.4)$$

where $H(t)$ denotes Heaviside's unit function. Accordingly, we have an operational equation

$$i(t)=A\frac{\alpha I(p)}{p+\alpha}H(t), \quad \cdots\cdots(3.5)$$

substituting (3.4) in (3.1).

Hence, in the same way as in the studies on the solutions of operational equations in Chapters IV, V and VI, we get the solution of (3.5) as follows;

$$i(t)=A\frac{q^3}{2}\left[-\left\{1+\frac{3}{4\pi\sigma\alpha q^2a^2}(\sqrt{4\pi\sigma\alpha}qa\coth\sqrt{4\pi\sigma\alpha}qa-1)\right\}e^{-\alpha t}\right.$$
$$\left.+\frac{6\alpha}{\pi^2}\sum_{s=1}^{\infty}\frac{1}{s^2}\frac{e^{-\alpha_s t}}{\alpha-\alpha_s}\right], \quad \cdots\cdots(3.6)$$

where α_s's are the successive roots of $\sin\sqrt{4\pi\sigma p}\,qa=0$ except zero. A more convenient expression for the small value of t is also obtained as follows. Taking into consideration the asymptotic expansion of F_0/F_1 given in (3.15), Chapter II, (3.5) can be written as

$$i(t)\simeq\alpha A\frac{q^3}{2}\left\{1-\frac{3}{\sqrt{4\pi\sigma}qa}p^{-\frac{1}{2}}+\frac{3}{4\pi\sigma q^2a^2}p^{-1}\cdots\right\}(p+\alpha)^{-1}H(t)$$
$$\simeq A\frac{q^3}{2}\left\{\frac{\alpha}{p+\alpha}+\frac{3}{4\pi\sigma q^2a^2}\left(\frac{1}{p}-\frac{1}{p+\alpha}\right)\right.$$
$$\left.-\frac{3}{\sqrt{4\pi\sigma}qa}(\alpha p^{-\frac{3}{2}}-\alpha^2p^{-\frac{5}{2}}+\cdots)\right\}H(t).$$

Then the solution of this operational equation becomes

$$i(t)\simeq A\frac{q^3}{2}\left[1-e^{-\alpha t}-\frac{3}{4\pi\sigma\alpha q^2a^2}(1-\alpha t-e^{-\alpha t})\right.$$
$$\left.-\frac{4}{\sqrt{4\pi\sigma\alpha}qa}\sqrt{\frac{\alpha^3t^3}{\pi}}\left\{1-\frac{2}{5}\alpha t+\cdots\cdots\right\}\right] \quad \cdots\cdots(3.7)$$

for the small value of t.

With the aid of (3.6) or (3.7), $i(t)$ is estimated for several values of σ as shown in Fig. 43 whereas A is assumed to be 21 *gammas* corresponding to the mean magnitude of sudden commencements given in Table XXIV. It was assumed, besides, that $a=6400\,km$, $\alpha=0.04\,sec.^{-1}$ and $q=1$.

As seen in the figure, the decay in the internal part becomes faster with decrease in conductivity, while the maxima in $e+i$ or ΔH occur 2 or 3 *minutes* after the beginnig. The ratio e/i amounts to about 4, 2.5 and less for $\sigma=10^{-15}$, 10^{-14} and 10^{-13} *emu* respectively at that moment. Comparing these values to that obtained from the analysis, it is reasonable to conclude that the conductivity in the earth approximately amounts to the order of 10^{-15} *emu*. Even if we take $q=0.9$, which is smaller than the determined value of q in the studies on the electromagnetic induction by various variations, σ hardly amounts to more than 10^{-14} *emu* for the explanation of the ratio.

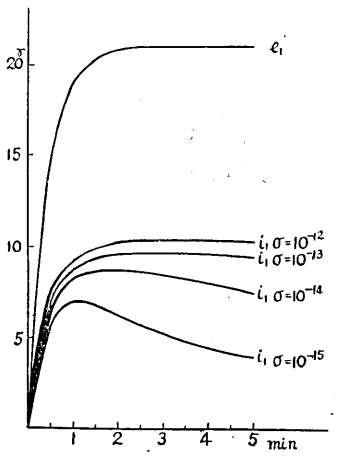

Fig. 43. The inducing and induced field for various cases.

The discrepancy between the electrical state of the earth obtained in the previous chapters in which σ amounts to $10^{-12}\sim10^{-13}$ *emu* below the depth of a few hundred *kilometers* and that obtained here is considerable, so that, taking into consideration the fact that the slower the change is the deeper the induced currents penetrate, we may presume the electrical conductivity near the earth's surface to be rather small because the greatest part of currents induced by sudden commencements flow in shallower zone than the induced currents in the cases of any other variation studied before. Hence, even in the superficial non-conducting layer reported in the studies of S_q, S_D, D_{st}, bay and magnetic variation connected with Dellinger effect, it is better to consider that the conductivity, though very low, has a finite value comparable with that of usual rock found on the earth's surface.

4. The distribution of the induced currents in the earth.

In order to examine the extent to which the induced currents penetrate, we shall study the distribution of the induced currents in the earth. The process of the calculation is just the same with Chapman and Prices'[8] investigation in the case of induction by D_{st} in which the components of the current-density are given by

$$c_r=0,\ c_\theta=0,\ c_\phi=-\sigma a\rho pC(p)F_1(k\rho a)e(t)P_1(\cos\theta),\quad \text{.....(4.1)}$$

where $$\rho=r/a$$

and $$C(p)=\frac{1}{2}\frac{1}{F_0(kqa)}\quad \text{.....(4.2)}$$

as already mentioned in Section 4, Chapter V.

Substituting (3.4) and (4.2) in (4.1), we get

$$c_\phi(t) = -\frac{A\sigma a\alpha\rho}{2}\frac{p}{p+\alpha}\frac{F_1(k\rho a)}{F_0(kqa)}H(t). \quad \text{.....(4.3)}$$

The solution of this operational equation is easily obtained as follows;

$$c_\phi(t) = -\frac{A\sigma a\alpha\rho}{2}\left[e^{-\alpha t}\left\{\frac{F_1(k\rho a)}{F_0(kqa)}\right\}_{p=-\alpha} + 2\sum_{s=1}^{\infty}(-1)^{s+1}\frac{\alpha_s e^{-\alpha_s t}}{\alpha-\alpha_s}\{F_1(k\rho a)\}_{p=-\alpha_s}\right] \quad \text{.....(4.4)}$$

After two or three *minutes* past from the beginning the first term in the bracket of the righthand side of (4.4) almost decays out getting

$$c_\phi(t) = \frac{3A}{4\pi a\rho}\sum_{s=1}^{\infty}(-1)^s\frac{\alpha}{\alpha-\alpha_s}\left(\cos\sqrt{4\pi\sigma\alpha_s}\rho a - \frac{\sin\sqrt{4\pi\sigma\alpha_s}\rho a}{\sqrt{4\pi\sigma\alpha_s}\rho a}\right)e^{-\alpha_s t}. \quad \text{.....(4.5)}$$

Taking $t=180\,sec.$ and $\sigma=10^{-15}\,emu$ the distribution of the induced currents are shown in Fig. 44 against depth in arbitrary unit. $\rho^3|c_\phi|$, which is proportional to the contribution of the currents in an infinitesimally thin layer of radius ρa to the magnetic field at the earth's surface, is also shown in Fig. 45. As shown

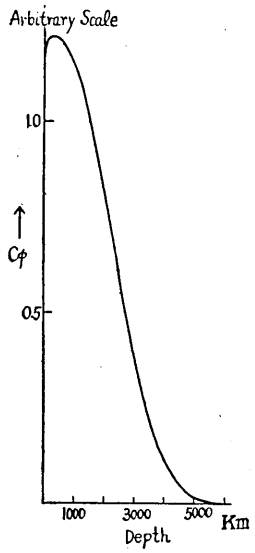

Fig. 44. The distribution of the induced currents in the earth.

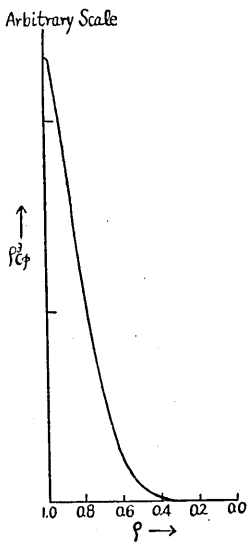

Fig. 45. The contribution of the induced currents to the magnetic field at the earth's surface.

in the figure, the contribution of the currents flowing in great depth is very small.

As will be discussed in the following Section, however, rapid variation such as sudden commencement is affected rather seriously by the presence of sea. Especially, in case of the distribution of the induced currents, we naturally presume that a considerable part may concentrate in the high conducting sea-water and consequently the remaining part which penetrates into the earth's interior becomes smaller than the estimate as mentioned above. Unfortunately, however, exact study is impossible owing to the irregular distribution of land and sea. In order to get some knowledge on the degree of partition of the induced currents in sea-water and the earth's interior, the writer assumes, as already done by Chapman, Price and Lahiri, that the earth is surrounded by a sea of uniform depth. In that case, regarding the sea as a thin, conducting shell having conductivity σ_0, depth D and radius a, the current-function J, as already obtained in (1.4), Chapter II, satisfies the next differential equation

$$\frac{1}{\sin\theta}\left\{\frac{\partial}{\partial\theta}\left(\sin\frac{\partial}{\partial\theta}\right)+\frac{1}{\sin\theta}\frac{\partial^2}{\partial\phi^2}\right\}J=a^2D\sigma_0\frac{\partial B_r}{\partial t}, \quad \text{.....(4.6)}$$

where B_r denotes the normal component of magnetic induction. When J and B_r can be expressed by series involving spherical surface harmonic S_n^m such as

$$\left.\begin{aligned} J&=\sum_n\sum_m K_n^m(t)\,S_n^m,\\ B_r&=\sum_n\sum_m M_n^m(t)\,S_n^m,\end{aligned}\right\} \quad \text{.....(4.7)}$$

we get from (4.6) by equating the corresponding terms of both sides

$$K_n^m=-\frac{a^2D\sigma_0}{n(n+1)}\frac{dM_n^m}{dt}. \quad \text{.....(4.8)}$$

In the case $n=1$, $m=0$, it becoms

$$K_1^0=-\frac{a^2D\sigma_0}{2}\frac{dM_1^0}{dt} \quad \text{.....(4.9)}$$

and using (1.3), Chapter II, the components of current-density are given by

$$c_\theta=0, \quad c_\phi=\frac{aD\sigma_0}{2}\frac{dM_1^0}{dt}P_1(\cos\theta). \quad \text{.....(4.10)}$$

Meanwhile the magnetic potential due to this shell is given by

$$\left.\begin{aligned} W_e&=\ 4\pi\sum_n\sum_m\frac{n}{2n+1}K_n^m S_n^m,\\ W_i&=-4\pi\sum_n\sum_m\frac{n+1}{2n+1}K_n^m S_n^m,\end{aligned}\right\} \quad \text{.....(4.11)}$$

respectively just out- and inside of the shell. Putting (4.8) in (4.11), we get for $n=1$, $m=0$

$$\left.\begin{aligned} W_e &= -\frac{2}{3}\pi a^2 D\sigma_0 \frac{dM_1^0}{dt}, \\ W_i &= \frac{4}{3}\pi a^2 D\sigma_0 \frac{dM_1^0}{dt}. \end{aligned}\right\} \quad \cdots\cdots(4.12)$$

Hence, taking into consideration that the magnetic potential of the variation is composed of the one due to this current-sheet and that due to the currents flowing inner region, we get for the case $n=1$, $m=0$

$$\left.\begin{aligned} ae &= ae' - W_i, \\ ai &= ai' + W_e, \end{aligned}\right\} \quad \cdots\cdots(4.13)$$

where e and i denote, as often used in this paper, the coefficients of the magnetic potential originating out- and inside of the suface and e' and i' the respective coefficients just below the sea considered. As shown by (2.1), since $M_1^0=-(e-2i)$, (4.13) can be written as

$$\left.\begin{aligned} e' &= e - \frac{4\pi a D\sigma_0}{3}\frac{d}{dt}(e-2i), \\ i' &= i - \frac{2\pi a D\sigma_0}{3}\frac{d}{dt}(e-2i). \end{aligned}\right\} \quad \cdots\cdots(4.14)$$

Then considering (3.1) and (3.2), e' is given by the operational equation as follows;

$$e'(t) = \left[1 - \frac{4}{3}\pi a D\sigma_0 p\{1-2I(p)\}\right] e(t). \quad \cdots\cdots(4.15)$$

Further, taking into account (3.4), we get

$$e'(t) = \frac{A\alpha}{p+\alpha}\left[1 - \frac{4}{3}\pi\alpha D\sigma_0 p\{1-2I(p)\}\right] H(t). \quad \cdots\cdots(4.16)$$

Then the current-density becomes for the inner region

$$c_{\phi\text{earth}} = -\sigma a\rho p C(p)\left[1 - \frac{4}{3}\pi a D\sigma_0 p\{1-2I(p)\}\right] \times \frac{A\alpha}{p+\alpha} F_1(k\rho a) H(t) P_1, \quad \cdots\cdots(4.17)$$

using e' in place of e in (4.1), while we also get for our sea from (4.10)

$$c_{\phi\text{sea}} = -\frac{aD\sigma_0 p}{2}\{1-2I(p)\}\frac{A\alpha}{p+\alpha} H(t) P_1. \quad \cdots\cdots(4.18)$$

By solving the operational equations (4.17) and (4.18), we get the whole distribution of the induced currents.

The solution for the small value of t is obtained as follows. Putting $q=1$, the coefficients of P_1 in (4.17) and (4.18) for the large value of p are written respectively

$$c_{\text{sea}}\ (t)\simeq -\frac{\alpha A}{4}\frac{3}{\sqrt{\pi\sigma}}(p^{-\frac{1}{2}}-\alpha p^{-\frac{3}{2}}\ldots)\,H(t)\,, \qquad \ldots\ldots\ldots\ldots(4.19)$$

$$c_{\text{earth}}(t)\simeq -\frac{\alpha A}{4}\frac{3}{\sqrt{\pi\sigma}}\frac{a}{\rho}\,p^{-\frac{1}{2}}e^{-\sqrt{4\pi\sigma}\,a(1-\rho)p^{\frac{1}{2}}}\left(1-2\sqrt{\frac{\pi}{\sigma}}\,D\sigma_0 p^{\frac{1}{2}}\ldots\right)H(t)\,. \qquad \ldots\ldots\ldots\ldots(4.20)$$

Applying the formulae of operational calculus, the solution of these equations are easily obtained for small t getting

$$c_{\text{sea}}\ (t)\simeq -\frac{\alpha A}{2}\frac{3}{\pi\sqrt{\sigma}}D\sigma_0 t^{\frac{1}{2}}\,, \qquad \ldots\ldots\ldots\ldots(4.21)$$

$$c_{\text{earth}}(t)\simeq -\frac{\alpha A}{2}\frac{3}{\pi\sqrt{\sigma}}\frac{a}{\rho}\,\sigma\left\{t^{\frac{1}{2}}\,e^{-\frac{\pi\sigma a^2(1-\rho)^2}{t}}\right.$$
$$\left.-\pi\sqrt{\sigma}a(1-\rho)\left(1-\text{erf.}\,\frac{\sqrt{\pi\sigma}a\,(1-\rho)}{t^{\frac{1}{2}}}\right)\right\}. \qquad \ldots\ldots\ldots(4.22)$$

Roughly speaking, then, the current-density in the sea is σ_0/σ times larger compared with that in the earth at $\rho=1$. As σ_0/σ amounts to as much as the order of 10^4, we know that the greatest part of the induced currents are flowing in sea-water. For illustration, current-distribution and its contribution to the field at the surface are shown in Figs. 46 and 47 for the case $\sigma=10^{-15}$ *emu*,

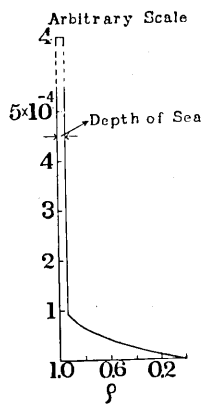

Fig. 46. The partition of the induced currents in the idealized sea and in the earth.

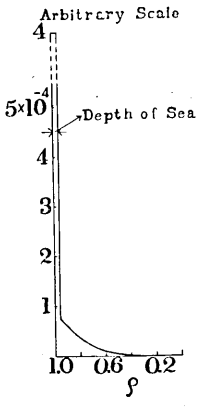

Fig. 47. The contribution of the induced currents in the idealized sea and in the earth to the magnetic field.

$\sigma_0=4\times10^{-11}$ *emu* and $t=3$ *minutes*. Although the present calculation seems to be an over-estimate on acount of its neglect of ocean boundaries, we may say that the conductivity obtained in this chapter is reliable as regards the shallow part of the earth.

5. The influences of the oceans.

Since, in the case of sudden commencement of magnetic storm, the rate of time-change in the earth's magnetic field is considerably larger than in the cases of any other variations treated in the preceding chapters, the electric currents induced in sea-water in which the conductivity amounts to the order of 10^{-11} *emu* will become more intense than the currents induced by more slower variations. In order to study, to what extent the magnetic field of sudden commencement may be affected by the presence of the oceans, we shall, in similar way with the study in the case of S_q, estimate the order of the magnetic field produced by the currents flowing in a sea bounded by two meridians $\pi/2$ apart in longitude.

The current-function J in such a sea with uniform depth D is already obtained in (1.4), Chapter II, being given by the solution of

$$\frac{1}{\sin\theta}\left\{\frac{\partial}{\partial\theta}\left(\sin\theta\frac{\partial}{\partial\theta}\right)+\frac{1}{\sin\theta}\frac{\partial^2}{\partial\phi^2}\right\}J=a^2D\sigma_0\frac{\partial B_r}{\partial t}, \quad \text{.....(5.1)}$$

where a, σ_0 and $\frac{\partial B_r}{\partial t}$ denote respectively the radius of the earth, specific conductivity of sea-water and flux-change per unit area. When J can be expressed by a series of the type

$$J=\sum_n\sum_m K_n^m S_n^m, \quad \text{.....(5.2)}$$

where $S_n{}^m$ denotes spherical surface harmonic and $K_n{}^m$ a function of time, we have

$$-\sum_n\sum_m K_n^m n(n+1) S_n^m=a^2D\sigma_0 f'(t) P_1, \quad \text{.....(5.3)}$$

where it is assumed

$$B_r=f(t) P_1(\cos\theta), \quad \text{.....(5.4)}$$

taking into consideration the distribution of the field of sudden commencement. Meanwhile, the normal component of the electric currents must vanish at the boundries, namely $i_\phi=0$ at $\phi=0$ and $\phi=\pi/2$. This condition is satisfied by taking $P_n{}^{2m}\sin 2m\phi$ in place of $S_n{}^m$. Then expanding P_1 into a series of the type

$$P_1=\sum_n\sum_m \gamma_{n,m} P_n^{2m} \sin 2m\phi \quad (0<\phi<\pi/2) \quad \text{.....(5.5)}$$

where $$\gamma_{n,m}=\frac{2n+1}{\pi}\int_{\theta=0}^{\pi}\int_{\phi=0}^{\pi/2} P_1 P_n^{2m} \sin 2m\phi \sin\theta \, d\theta d\phi\,, \quad \text{.....(5.6)}$$

we get K_n^m by comparing the corresponding coefficients of both sides of (5.3) as follows;

$$K_{2k+1}^{2l+1}=-a^2D\sigma_0 f'(t)\frac{\gamma_{2k+1,2l+1}}{(2k+1)(2k+2)} \quad \text{.....(5.7)}$$

because $\gamma_{2k,2l+1}$, $\gamma_{2k,2l}$ and $\lambda_{2k+1,2l}$ are all zero. $\gamma_{2k+1,2l+1}$ is easily calculated from (5.6). Substituting, then, (5.7) in (5.2), the current-function can be expressed by

$$J=-a^2D\sigma_0 f'(t)\sum_{k=1}^{\infty}\sum_{l=0}^{l\leq\frac{k-1}{4}}\frac{\gamma_{2k+1,2l+1}}{(2k+1)(2k+2)} P_{2k+1}^{2(2l+1)} \sin 2(2l+1)\phi\,, \quad \text{(5.8)}$$

or taking main term we have

$$J=-a^2D\sigma_0 f'(t)\{(0.0925\,P_3^2+0.0232\,P_5^2+\ldots)\sin 2\phi+\ldots\} \quad \text{.....(5.9)}$$

by which we can draw the current-lines in our ocean as shown in Fig. 48. The amount of the current-flow between two adjacent lines in the figure is constant.

In order to estimate the magnetic field produced by the electric currents shown in the figure, let us use an approximate method. Though (5.8) or (5.9) are merely available in the region $0<\phi<\frac{\pi}{2}$, we assume that they are effective all over the earth neglecting the magnetic field produced by the currents flowing in the rgeions except $0<\phi<\pi/2$, whence the magnetic potential due to these currents flowing in a spherical shell is given by

$$W=4\pi\sum_n \frac{n}{2n+1} J_n (a/r)^{n+1} \quad \text{.....(5.10)}$$

out of the earth, where J_n denotes the term of the current-function having order n.

Thus, differentiating W with respect to the respective directions, the components of the magnetic field at $r=a$ are approximately given as follows;

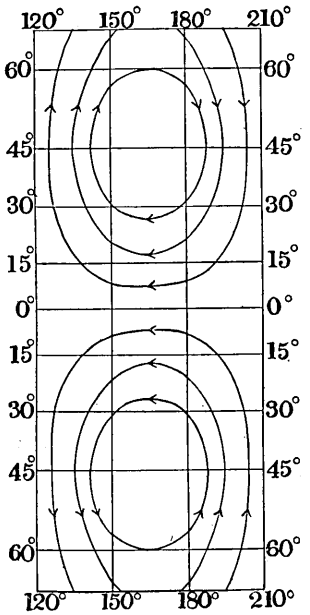

Fig. 48. The induced currents in the ocean.

$$X=1.49\,aD\sigma_0 f'\,(X_3^2+0.443\,X_5^2+\ldots)\sin 2\phi\,, \quad \ldots\ldots\ldots\ldots(5.11)$$

$$Z=1.98\,aD\sigma_0 f'\,(P_3^2+0.400\,P_5^2+\ldots)\sin 2\phi\,. \quad \ldots\ldots\ldots\ldots(5.12)$$

Hence the magnetic field on $\phi=45°$ meridian becomes as shown in Fig. 49 in which the increase in Z near the centre of eddies in Fig. 48 is remarkable.

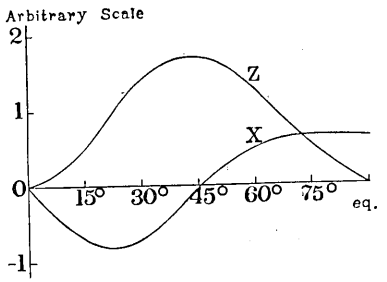

Fig. 49. The magnetic field produced by the induced currents in the ocean.

As an accurate estimate is difficult to get owing to the ambiguity of the determination of the flux-change or $f'(t)$, we shall estimate very roughly the order of the field-intensity. Taking $a=6400\,km$, $D=4000\,m$, $\sigma_0=4\times10^{-11}emu$ and $f'=10^{-3}\gamma/sec$, Z near the centres of eddies amounts to about 20 *gammas*, downwards or upwards respectively in the northern or southern hemispheres, while H amounts to about 8 *gammas*, northwards, on the equator.

With such effect of ocean in mind, it may fairly be presumed that Honolulu, situated in the northern part of the central Pacific Ocean, is affected remarkably in vertical intensity as shown in Fig. 42 deviating about 10 *gammas* from the normal distribution. Such effect is likely to exist in the case of Porto Rico though mathematical investigation is more difficult to carry out.

As mentioned in the well known book "*Geomagnetism*",[67] the sign of ΔZ on different occasions at the same station is roughly constant, though not so constant as for ΔH. But, the opposition of sign between the values of ΔZ at relatively near stations, for example Greenwich and Paris, is striking and almost invariable, though in ΔH and ΔD the movements are generally the same. The opposition of sign is only observable in the case of sudden change. Hence it is possible to attribute such phenomena to the local characters of which the distribution of sea is probably the most important factor.

As already mentioned in this section, the influences of sea on sudden changes in the earth's magnetic field are sometimes striking, but it is difficult to discuss in detail on account of the irregular distribution of land and sea.

---

67) CHAPMAN and BARTELS, *loc. cit.* Vol. I, p. 297.

SUMMARY AND CONCLUSION

In Chapter I, brief outlines of the investigations carried out up to this time on the magnetic permeability in the earth were described. These studies, both physical and geophysical, proved the ferromagnetic state in the earth to be impossible. Although the results of these studies are not always applicable to the actual earth, we may consider, at the present stage of investigation, that the magnetic permeability does not differ materially from unity. For this reason, the writer assumed $\mu=1$ throughout this study.

In the first part of Chapter II, the influences of oceans on the diurnal variation on quiet days were discussed. Since the specific conductivity of sea-water amounts to the order of 10^{-11} *emu*, about 10,000 times larger than that of usual rocks found on the earth's surface, the electric currents induced by magnetic variation in deep ocean will become appreciably intense. In practice, the magnetic field produced by the oceanic-current will be of complicated distribution corresponding to the irregular distribution of land and sea. Owing to mathematical difficulties, only a few investigations on the effect of world-wide ocean of uniform depth spread all over the earth were hitherto carried out. The writer, intending to study the possible effect of oceans, such as the Pacific and the Atlantic, investigated to what extent S_q might be affected by the presence of a sea of uniform depth bounded by two meridians $\pi/2$ apart in longitude. The results indicated that S_q might not be so affected by the ocean that the field due to induced currents in the ocean occupies the main part. Accordingly, the internal part of S_q obtained from spherical harmonic analysis in which it was assumed that S_q depends solely on local time could be on the whole considered for that was produced by the induced currents flowing in the inner part of the earth. Further, on certain assumptions, though not quite accurate, the effect of the Pacific Ocean was abstracted which agreed roughly with what was expected from the theory. As to the layer of moist soil covering the land area, its influence is negligible because its conductivity is less than 1/100 of sea-water and its thickness does not exceed 1000 *m*.

In the succeeding sections of Chapter II, electromagnetic induction by S_q was studied with the aid of a newly made analysis. As Nagata pointed out, the analyses made by Hasegawa and Benkova seem to be more reliable than the well known Chapman's analysis which has been hitherto used to study electromagnetic induction by S_q. Taking into consideration the discontinuity at the depth of 2900 *km*, the writer attempted to determine the electrical state out- and inside of this boundary separately. Unfortunately, however, the induced currents do not always penetrate into great depth, and the determined con-

ductivity for the inner core was ambiguous though we got a value about ten times larger than the outer part or mantle. Hence, the result agreed with that obtained in the case of uniform core model. We get, as already obtained by Nagata, $\sigma=5.0\times10^{-12}$ *emu* and the depth of non-conducting layer $D=400$ *km* on the basis of Benkova's analysis while Chapman has obtained $\sigma=3.6\times10^{-13}$ *emu* and $D=260$ *km* from his own analysis. It is of interest that the conductivity obtained from the newly made analysis becomes about ten times larger than that obtained from Chapman's old one.

Recent accumulation of magnetic data shows clearly that there were, on the average, daily variation of definite type on disturbed days called solar daily disturbance variation or S_D. As shown empirically by Chapman and theoretically by the preseht writer, the distribution of S_D differs very much from that of S on quiet days or S_q. In order to check the electrical state of the earth's interior obtained from the study of S_q, electromagnetic induction by S_D was studied in Chapter III. Though it was impossible to make an accurate determination on account of the shortage of available data, we found out that the electrical state for S_q was approximately applicable to the electromagnetic induction by S_D.

In Chapter IV, electromagnetic induction by storm-time variation or D_{st} within the earth-model consisting of superficical non-conducting layer, mantle and inner core, was studied with a view to getting some knowledge about the electrical state in deeper region. Since the conductivity amounts to 5×10^{-12} *emu* in Benkova's model, the discrepancy between the studies on S_q and D_{st} which was hitherto taken into account seriously by Chapman and his colleagues was almost overcome leaving little difference. Although, the remaining difference was vanished by introducing high conducting inner core as obtained in the case of S_q, the value of the conductivity was less reliable because only a minor part of the induced currents penetrates into such region of great depth.

With the aid of Hatakeyama's excellent data, the writer treated the electromagnetic induction by bay-type disturbance in Chapter V. Separation of the external part from the internal one was carried out after the same method as in the case of D_{st}. With the idealized feature of the atmospheric current-systems obtained both empirically and theoretically in mind, only the coefficients of $Q_1^1(\cos\theta)$, which was the most predominant in the magnetic potential in the low and middle latitudes, were studied. Roughly speaking, the results supported the view obtained in the studies on S_q. The electrical conductivity must increase below the depth of a few hundred *kilometers* from the earth's surface amounting at least to the order of 10^{-12} *emu*. The extent to which the induced currents penetrate was also studied, the conclusion being

that they become practically zero at the depth of several hundred *kilometers* measured from the earth's surface. Considering the duration-time of bay-type disturbances which amounts to 1~5 *hours*, the obtained conductivity should be reliable as to regions shallower than those in the case of S_q and of course D_{st}.

Moreover, we have a type of variation of shorter duration. That is the magnetic effect connected with solar eruption and consequently with radio fade-out or Dellinger effect. Electromagnetic induction by magnetic variation of this type was studied in Chapter VI. As has been made clear recently, since the magnetic effects accompanying the solar eruption are an augumentation of diural variation departure having no effect in the dark hemisphere, a larger number of observed data from well-distributed observatories are needed for spherical harmonic analysis. However, we lack sufficient data for the purpose. Then, the writer treated the problem as an induction within plane-earth in the European Region where the distribution of observatories is comparatively dense. Constructing the theory of plane-earth induction, the writer investigated the electrical state of the earth's interior inferred from the variation and found out that the conductivity increased below the depth of 400 *km* amounting to 10^{-12} *emu* while the outer layer must be non-conducting. Though only an example from Birkeland's data was available and we could say nothing about the accuracy of determination, it was of interest to note that the result agreed with the view in the cases of various variation treated in the previous chapters. The induced currents decrease very sharply with the increase of depth, the determined conductivity corresponding to that just below the boundary between the non-conducting and conducting regions.

In Chapter VII, induction by sudden commencement of magnetic storm, one of the most rapid variation in the earth's magnetic field, was discussed. As shown in the last section, since sudden commencement are apt to be affected by the complicated influence of sea, the discussions seem to be rather rough. Treating in the same way as in the study in previous chapters, however, we got, on the average, the ratio of the coefficient of the external potential to that of the internal one amounting to as much as 3.9 for $P_1(\cos\theta)$. Such a large value was hardly to be expected from the earth-model in the cases of the variations treated before. A plausible explanation was furnished by taking the conductivity of the earth to be as small as 10^{-15} *emu* agreeing with that of usual rocks found on the earth's surface. Hence, taking into consideration the sharp decrease of the induced currents with the increase of depth, especially concentration in sea, we concluded that even in the non-conducting region obtained in the studies on S_q, D_{st}, bay and variation connected with solar eruption the conductivity took a finite value of the order of 10^{-15} *emu*.

Table XXVII Summarization of the

Variation	Pericd or approximate duration-time	Researcher	Data	e/i at maximum variation
Diurnal variation on quiet days (S_q)	24 and 12 *h.* (Auxiliary 8 and 6 *h.*)	Chapman and Price	Chapman	2·8 for P_2^1, 2·2 for P_3^2
		Lahiri and Price	,,	——
		Terada	,,	——
		Nagata	Hasegawa	2·30 for P_2^1, 2·43 for P_3^2
		Nagata	Benkova	2·34 for P_2^1, 2·30 for P_3^2
		Riki.ake	Chapman	——
		Rikitake	Benkova	——
Solar daily disturbance variation (S_D)	24 *h.*	Rikitake	Vestine	3·7 for P_2^1, 2·3 for P_4^1
Storm-time variation (D_{st})	2~3 *days*	Chapman and Price	Chapman	2·4 for P_1
		Lahiri and Price	,,	——
		Nagata	,,	——
		Rikitake	,,	——
Bay-type disturbance	1~3 *h.*	Rikitake	Hatakeyama	2·2 for Q_1^1
Variation connected with solar eruption	30 *min.*	Rikitake	Birkeland	2·4 for wave length approximately 6000 *km.*
Sudden commencement of magnetic storm	3 *min.* (average)	Rikitake	Bauer	3·9 for P_1

electrical state of the earth's interior.

Electrical state		Effective depth (*km*)	Remark
Depth (*km*)	Conductivity (*emu*)		
250	3.6×10^{-13}	700*)	
Conductivity increases with increases of depth.		——	Non-uniform earth
	"	——	Non-uniform earth
400	1.5×10^{-12}	850*)	
400	5.1×10^{-12}	850*)	
200	3.0×10^{-13} (3×10^{-11} for inner core)	——	Earth-model consisting of mantle and inner core
400	5.0×10^{-12} (5×10^{-11} for inner core)	850*)	"
Roughly agrees with S_q.		——	
400	4.4×10^{-12}	1100	
700	more than 10^{-11}	——	Non-uniform earth
400	5.1×10^{-12}	1100	
400	5.0×10^{-12} (5×10^{-11} for inner core)	1100	Earth-model consisting of mantle and inner core
260	at least 10^{-12}	320	
400	10^{-12}	420	Plane-earth
0~500	10^{-15}	30**)	Accurate determination for both depth and conductivity is unable.

*) Mean for P_2^1 and P_3^2.

**) It was assumed that the earth was covered by world-wide sea, a few thousand *meters* in depth.

Toward the end of this chapter, possible influence of any ocean on sudden commencement was discussed to obtain results for a reasonable explanation of abnormality in vertical intensity at observatories situated in ocean. According to the writer's opinion, sudden changes in the earth's magnetic field are sometimes affected considerably by the presence of sea though exact investigation is of great difficulty to carry out on account of the irregular distribution of land and sea.

In addition to various variations treated in this paper, we have a kind of magnetic variation of special type called pulsation. Unfortunately, however, as the writer has no data available yet, the electromagnetic induction by pulsation will be left untouched till he can get sufficient data.

Summarization of the results of this paper is shown in Table XXVII together with those hitherto obtained by many researchers. The depth and conductivity tabulated in this Table were obtained with respect to the uniform core model excepting the studies done by Lahiri and Price, and Terada.

The writer introduced a convenient concept "effective depth" in order to get the distribution of the electrical conductivity in the earth. As mentioned in the respective sections of all chapters, we know the distribution of the induced currents in the conducting region and consequently the contribution

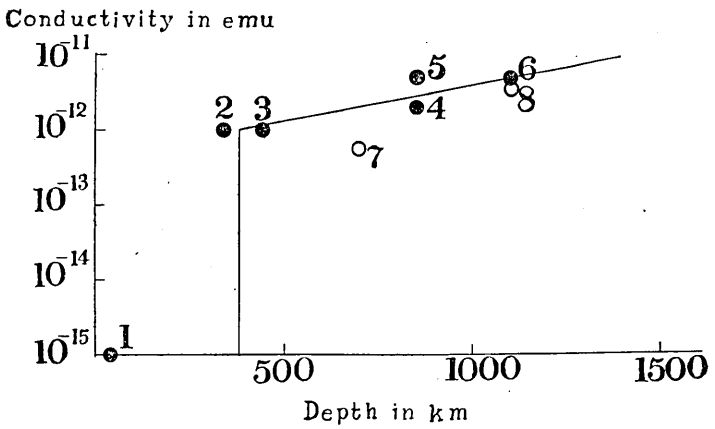

Fig. 50. The conductivity-distribution in the earth.
1. Sudden commencement.
2. Bay-type disturbance.
3. Variation connected with solar eruption.
4. S_q (Hasegawa).
5. S_q (Benkova).
6. Dst (Chapman-Benkova).
7. S_q (Chapman).
8. Dst (Chapman).

of current flowing at any depth to the magnetic field at the earth's surface as a function of depth denoted by $\varphi(D)$ or $\varphi(\rho)$ in the spherical case. We shall define the most effective depth that coresponds to the determined conductivity by $\int D\varphi(D)\,dD \Big/ \int \varphi(D)\,dD$ or $\int_0^1 \rho\varphi(\rho)\,d\rho \Big/ \int_0^1 \varphi(\rho)\,d\rho$ in the spherical case. With the aid of these expressions, the writer calculated "effective depth" in each case as shown in Table XXVII. Hence the conductivity can be plotted against depth, though not exactly, as shown in Fig. 50. Taking into consideration the fact that the conductivity of usual rocks found on the earth's surface amounts to the order of as small as 10^{-15} *emu*, the increase of the conductivity must be so steep, almost discontinuous, down to the depth of about 400 *km*. Then the rate of increase becomes small. The electrical state in great depth, more than 1500 *km*, can not be accurately determined though it seems advantageous for the explanation of the electromagnetic induction by D_{st} that the greater the depth the higher the conductivity.

It is beyond the scope of the present paper to investigate into the reason why the conductivity increases enormously below the depth of a few hundred *kilometers*. It must be discussed from the physical stand-point. The writer hopes that studies on the properties of matter under high pressure and high temperature will give, in the near future, some suggestions for the interpretation of the results given in the present study.

ACKNOWLEDGEMENT

In the course of this study, the writer was encouraged by his senior colleagues, among whom to Professor C. Tsuboi and Dr. T. Nagata especially the writer wishes to express his cordial thanks for their kind advices and helpful suggestions. At the same time the writer also wishes to express his hearty thanks to Professor F. Kishinouye, Professor T. Hagiwara and Professor T. Minakami who gave him the chance to carry out this study and offered him helpful criticisms. He also cordially expresses thanks to Dr. H. Hatakeyama for his kind suggestions on magnetic data.

Throughout the numerical work, Miss K. Sano always assisted the writer and to her the writer's hearty thanks are also due. A part of this study was done with the financial aid of research grant from the Department of Education and sincere thanks are also due to the Department.

APPENDIX

When the writer studied magnetic effect connected with solar eruption or Dellinger effect, it was treated as plane-earth induction owing to the shortage of well-distributed data. Though it is not unusual to regard a part of the

earth's surface as a plane in potential problem of geophysics, the influence of the neglect of the earth's curvature should be taken into account for the present problem because the induced currents which produce the internal part of the magnetic potential concentrate at the depth of several hundred *kilometers* which amounts to about one tenth of the earth's radius. From this point of view, the difference between the spherical and plane induction will be discussed here.

Taking the uniform core model, in the first place, the relations between the coefficients of spherical surface harmonics are obtained as follows. In general, the potential of the magnetic field can be expressed by

$$W=a\sum_{n=1}^{\infty}\sum_{m=0}^{n}\{e_{n,a}^{m}\rho^{n}+i_{n,a}^{m}\rho^{-n-1})\cos m\phi+ (e_{n,b}^{m}\rho^{n}+i_{n,b}^{m}\rho^{-n-1})\sin m\phi\}P_{n}^{m}$$

in polar coordinate where a, ρ, e and i denote respectively the earth's radius, radial distance divided by a, the coefficients of the potential originated above the earth and those originated in the earth. When, by means of spherical harmonic analysis, the northward and downward components of the magnetic field may be expressed as

$$X=\sum_{n=1}^{\infty}\sum_{m=0}^{n}(a_{n}^{m}\cos m\phi+b_{n}^{m}\sin m\phi)\,X_{n}^{m},$$

$$Z=\sum_{n=1}^{\infty}\sum_{m=0}^{n}(\tilde{a}_{n}^{m}\cos m\phi+\tilde{b}_{n}^{m}\sin m\phi)\,P_{n}^{m},$$

we have the well-known relations

$$a_{n}^{m}=n(e_{n,a}^{m}+i_{n,a}^{m}),\qquad \tilde{a}_{n}^{m}=ne_{n,a}^{m}-(n+1)\,i_{n,a}^{m},$$

$$b_{n}^{m}=n(e_{n,b}^{m}+i_{n,b}^{m}),\qquad \tilde{b}_{n}^{m}=ne_{n,b}^{m}-(n+1)\,i_{n,b}^{m}.$$

These relations can also be obtained from the combination of the eastward and downward components.

Meanwhile, according to the induction theory, the coefficients of internal origin are given by the operational equation

$$i_{n}^{m}(t)=I(p)\,e_{n}^{m}(t)$$

where $$I(p)=\frac{nq^{2n+1}}{n+1}\left\{1-\frac{F_{n}(k^{2}q^{2}a^{2})}{F_{n-1}(k^{2}q^{2}a^{2})}\right\},\quad k^{2}=4\pi\sigma p.$$

In the expressions, σ and q denote respectively the electrical conductivity and the radius of the conducting core. Magnetic permeability is assumed to be unity while F_n is a transcendental function which was already studied in

detail by S. Chapman and A. T. Price[8]. In the case of periodic induction of period $2\pi/\alpha$, we have i_n^m corresponding to $e_n^m = E_n^m \cos \alpha t$ as follows

$$i_n^m = \frac{nq^{2n+1}}{n+1} E_n^m \left\{ \left(1 - \frac{A}{A^2+B^2}\right)\cos \alpha t - \frac{B}{A^2+B^2} \sin \alpha t \right\},$$

where

$$A = \frac{\beta}{2n+1}\left\{1 + \frac{n}{\beta} + \frac{n(n+1)}{4\beta^2} \cdots\right\},$$

$$B = \frac{\beta}{2n+1}\left\{1 - \frac{n(n+1)}{4\beta^2} - \frac{n(n+1)}{4\beta^3}\right\}, \qquad \beta^2 = 4\pi^2 \sigma q^2 a^2 .$$

Thus we get

$$a_n^m = nE_{n,a}^m \left[\left\{1 + \frac{nq^{2n+1}}{n+1}\left(1 - \frac{A}{A^2+B^2}\right)\right\}\cos \alpha t - \frac{nq^{2n+1}}{n+1} \frac{B}{A^2+B^2} \sin \alpha t \right],$$

$$\tilde{a}_n^m = nE_{n,a}^m \left[\left\{1 - q^{2n+1}\left(1 - \frac{A}{A^2+B^2}\right)\right\}\cos \alpha t + q^{2n+1} \frac{B}{A^2+B^2} \sin \alpha t \right], \text{ etc.}$$

Hence, we can calculate the magnetic forces at the earth's surface corresponding to any magnetic potential of external origin.

Next, the magnetic forces are analysed in a rectangular area as shown in Fig. 51. We obtain $A_{\mu\nu}$ and $\tilde{A}_{\mu\nu}$ as the coefficients of $\sin \frac{\mu\nu}{L} x \cos \frac{\nu\pi}{L'} y$ in X and $\cos \frac{\mu\pi}{L} x \cos \frac{\nu\pi}{L'} y$ in Z. Meanwhile, as mentioned in Chapter VI, we have

$$e_{\mu\nu} = \frac{1}{2}\left\{ \frac{L}{\mu\pi} A_{\mu\nu} + \frac{1}{\pi\left\{\left(\frac{\mu}{L}\right)^2 + \left(\frac{\nu}{L'}\right)^2\right\}^{\frac{1}{2}}} \tilde{A}_{\mu\nu} \right\},$$

$$i_{\mu\nu} = \frac{1}{2}\left\{ \frac{L}{\mu\pi} A_{\mu\nu} - \frac{1}{\pi\left\{\left(\frac{\mu}{L}\right)^2 + \left(\frac{\nu}{L'}\right)^2\right\}^{\frac{1}{2}}} \tilde{A}_{\mu\nu} \right\}.$$

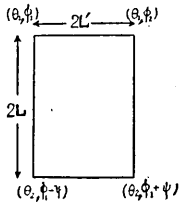

Fig. 51.

Then the coefficients of external and internal parts can be calculated in the case of plane-earth from the external potential given for spherical case.

On the other hand, according to the plane-earth induction theory studied in Chapter VI, the coefficients of internal origin $i'_{\mu\nu}$ are given by

$$i'_{\mu\nu}(t) = I'(p)\, e_{\mu\nu}(t),$$

where

$$I'(p) = e^{-2\pi\left\{\left(\frac{\mu}{L}\right)^2 + \left(\frac{\nu}{L'}\right)^2\right\}^{\frac{1}{2}} D} \times \frac{\left\{\pi^2\left[\left(\frac{\mu}{L}\right)^2 + \left(\frac{\nu}{L'}\right)^2\right] + 4\pi\sigma p\right\}^{\frac{1}{2}} - \pi\left\{\left(\frac{\mu}{L}\right)^2 + \left(\frac{\nu}{L'}\right)^2\right\}^{\frac{1}{2}}}{\left\{\pi^2\left[\left(\frac{\mu}{L}\right)^2 + \left(\frac{\nu}{L'}\right)^2\right] + 4\pi\sigma p\right\}^{\frac{1}{2}} + \pi\left\{\left(\frac{\mu}{L}\right)^2 + \left(\frac{\nu}{L'}\right)^2\right\}^{\frac{1}{2}}}.$$

In the expression, D denotes the depth of the non-conducting layer. When $e_{\mu\nu} = P\cos\alpha t + Q\sin\alpha t$, we get

$$i'_{\mu\nu}(t)=\frac{e^{-iuD}}{2\sqrt{\sqrt{u^4+v^2}+u^2}+2u\sqrt{\sqrt{u^4+v^2}u^2}}$$

$$\times\left[\left\{P(2\sqrt{u^4+v^2}-u^2)+2Qu\sqrt{\sqrt{u^4+v^2}-u^2}\right\}\cos\alpha t\right.$$

$$\left.-\left\{2Pu\sqrt{\sqrt{u^4+v^2}-u^2}-Q(2\sqrt{u^4+v^2}-u^2)\right\}\sin\alpha t\right],$$

where $$u=\pi\left\{\left(\frac{\mu}{L}\right)^2+\left(\frac{\nu}{L'}\right)^2\right\}^{\frac{1}{2}} \text{ and } v=4\pi\alpha\sigma .$$

To discuss the influence of plane-earth treatment, then, will be reduced to compare $i_{\mu\nu}$ to $i'_{\mu\nu}$.

For instance, a comparison in the case of induction by variation associated with solar eruption, will be approximately made as follows.

As is well known, the atmospheric current-systems of that variation closely resemble those of S_q in the sunlit hemisphere. For this reason, we may assume that the potential of the inducing field is given by

$$W=K\{7\cdot7\,P_2^1\cos(\phi+24^\circ)+4\cdot4\,P_3^2\cos(2\phi+202^\circ)$$
$$+2\cdot2\,P_4^3\cos(3\phi+35^\circ)+0\cdot7\,P_5^4\cos(4\phi+232^\circ)\}$$

that is proportional to the S_q current-systems obtained by Chapman as the equinoctial mean for the year 1905. Further, we assume that the field is periodic, say $K=K_0\cos\alpha t$, for the sake of mathematical simplicity. Thus calculating a_n^m and $\tilde{a}_n^m$, we get

$$X=K_0\cos\alpha t\{22\cdot6\,X_2^1\cos(\phi+24^\circ)+19\cdot3\,X_3^2\cos(2\phi+202^\circ)$$
$$+12\cdot6\,X_4^3\cos(3\phi+35^\circ)+4\cdot8\,X_5^4\cos(4\phi+232^\circ)\}$$
$$-K_0\sin\alpha t\{0\cdot3\,X_2^1\cos(\phi+24^\circ)+0\cdot3\,X_3^2\cos(2\phi+202^\circ)$$
$$+0\cdot3\,X_4^3\cos(3\phi+35^\circ)+0\cdot1\,X_5^4\cos(4\phi+232^\circ)\},$$
$$Z=K_0\cos\alpha t\{4\cdot6\,P_2^1\cos(\phi+24^\circ)+5\cdot2\,P_3^2\cos(2\phi+202^\circ)$$
$$+4\cdot1\,P_4^3\cos(3\phi+35^\circ)+1\cdot9\,P_5^4\cos(4\phi+232^\circ)\}$$
$$+K_0\sin\alpha t\{0\cdot4\,P_2^1\cos(\phi+24^\circ)+0.5\,P_3^2\cos(2\phi+202^\circ)$$
$$+0\cdot3\,P_4^3\cos(3\phi+35^\circ)+0\cdot1\,P_5^4\cos(4\phi+232^\circ)\},$$

where it is assumed that $\sigma=10^{-12}$ *emu*, $q=0.94$ and the period is 1 *hour*. Then neglecting the term involving $\sin\alpha t$ in which the coefficients are less than one tenth compared to the term involving $\cos\alpha t$, e_{10} and i_{10} are calculated with

respect to the meridian $\phi=165°$ that passes the centre of the current-systems. i_{10}/e_{10} is shown in Fig. 52 being plotted against L, half wave-length, that measured from $\theta=20°$ to the lower latitudes. i'_{10}/e_{10} is also calculated for $D=400\ km$ being also shown in Fig. 52. As seen in the figure, the discrepancy between i and i' becomes considerable as L becomes small. Hence it is dangerous to analyse in a region whose range does not exceed much the depth of the non-conducting layer. However, it seems likely that the treatment in Chapter VI, in which $L=3000\ km$ will be, to a rough approximation, correct.

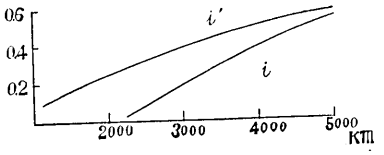

Fig. 52.

---

18. 地球内の電磁感應およびその地球内部の電氣的性質との關係 第1報 (2)

地震研究所 力武常次

太陽面爆發に伴う地磁氣變化（デリンジヤー現象に伴う變化）はまた極めて特徴のある變化の型式を示し，その分布は夜間の半球では變化を示さず，晝間の半球では日變化磁場を增大するような變化をすることがよく知られているが，第6章に於て Birkeland の集めた資料によつて，上述の各章に於けると同樣の考察を行つた．この場合球函數分析を行うためには高次の球函數をも考慮せねばならず，數少い觀測資料を使うためにやむをえず比較的觀測點の多いヨーロツパ地方に就いて，地球を平面的に取扱つた．方法は地球を球とした場合と同じであつて，波長 6000 *km* の調和函數に就いて內外磁場を分離した．この內外磁場間の關係はやはり絕緣的な表面層の深さを 400 *km*，それより下の部分では $\sigma=10^{-12}\ emu$ とすると都合よく說明出來る．

海型變化では變化の繼續時間は 1～3 時間，太陽面爆發に伴う變化では 30 分程度である．これに對し磁氣嵐の急始に於ては水平分力の飛躍は平均として 2～3 分程度で終了する．第7章は磁氣嵐の急始を取扱つたもので，資料は Bauer の集めたものによつた．Dst の場合と同樣中低緯度に於て P_1 の係數を求めた．この場合外および內側に原因を有する磁場のポテンシヤルの比は 3.9 程度となり，今迄扱つた變化のそれに比して著しく內部磁場が小さい．したがつて地球の最も外側に近い部分の σ が小さい（$10^{-15}\ emu$ 程度）ために短週期の變化ではこのようにあらわれるのではないかと考えられる．またこのようなはやい變化に對しては，海水の高電導性が問題となり，それについて若干の議論を行つた．

上述の各種の變化の資料の精度は一定ではなく，したがつて決定された電氣的性質の信賴度も一定でなく，誤差の評價も困難であるが一應かなりはやい變化からおそい變化迄を含んでいるか

ら，いろいろな深さについて σ の分布が如何様であるかの目安を近似的につくることが可能と思われる．一般に誘導電流の深さに對する分布したがつて任意の深さを流れる電流の表面磁場に對する寄與を計算することが出來るから筆者は最も有効な深さとして $\int D\varphi(D)\,dD/\int\varphi(D)\,dD$ で與えられる量をとつた．玆に $\varphi(D)$ は D なる深さのところを流れる電流の表面に於ける磁場に對する寄與を表わす．球として取扱つた場合は，$\int_0^1\rho\varphi(\rho)\,d\rho/\int_0^1\varphi(\rho)\,d\rho$ ($\rho=r/a$, a は地球の半徑) としてよい．卽ちこれ等の式で定義される深さの電氣的性質が決定された σ に對して最も有効であると考えるのであつて，一義的に決めることが不可能な以上この程度の近似的な考え方で滿足せざるを得ない．その結果は本文中の最後の圖に示したような σ の分布となつて，地表下 400 *km* 附近に殆ど不連續と考えられるような飛躍を考えねばならない．もし σ が岩石中のようにイオン傳導度によるとすると溫度の增加は σ を增し壓力の增大は σ を減少させる方向に働くと考えられるが，定量的なことは物理學的な物性に關する理論および高溫高壓下の實驗をまつて說明されるべきことがらであり，本報文に於ては單に地磁氣變化の研究より得られた結果を述べるにとゞめる．

またこのように σ の大體の分布を求め得たからには，第二の近似として σ がこのような分布をするモデルを考えて各種の地磁氣變化から分布型式をさらに精密に決定することが望ましいが，それは次の機會に實行したいと考える．